Inverse Problems for Stochastic Neutronics, considering two time gates

Corentin Houpert,[*,a] Josselin Garnier,[b] and Philippe Humbert[c]

[a] *University of Leicester*
University Road, Leicester LE1 7RH

[b] *CMAP*
Ecole Polytechnique
Route de Saclay
91128 PALAISEAU Cedex

[c] *CEA, DAM, DIF*
F-91297 Arpajon

[*]Email: chresearch.polytechnique@gmail.com

Number of pages: 43
Number of tables: 4
Number of figures: 16

Abstract

Fissile matter detection and characterisation are crucial issues; especially in nuclear safety, safeguards, matter compatibility, reactivity measurements. In this context, we want to identify a source of fissile matter knowing external measures such as instants of detection of neutrons during an interval of measure. Thus, we observe the neutrons detection times emitted by the fissile matter and going through the detector, then we compute the moments of the empirical distribution of the number of neutrons detected during a time gate T. In order to identify the source we have to get the following parameters: the multiplication factor k_{eff} of the system, the intensity of the source S, the fission efficiency ε_F.

Given the parameters of the source there are some models that allow us to predict the moments of counted number of neutrons during a time gate T. We consider a point model stating monokinetic neutrons are moving in an infinite, isotropic and homogeneous medium.

The method makes it possible to compute the first moments of the neutron counting distribution.

Then, given the moments of counted number of neutrons during a time gate T we want to get the parameters of the fissile source. In order to achieve this goal, we will use the following method

- Bayesian approach in order to get the distribution of parameters. The a posteriori distribution is non-trivial, samples can be achieved with Markov Chain Monte-Carlo methods with Covariance Matrix Adaptation (MCMC with CMA).

Finally, we will consider two time gates T_1 and T_2 in two complementary regimes of the first moments. For a time of measurements 3600s, it is already settled that the use of T_1 and T_2 provide a better sampling of the a posteriori distribution of the parameters knowing the measurements than with just T_1 or T_2. We also compare the sampling for the use T_1 for a time of measurements of 7200s and T_1 and T_2 for a time of measurements of 3600s. We concluded that using this larger time of measurements and T_1 provide a better sampling of the a posteriori distribution of interest than the use of the smaller time of measurements T_1 or T_2. Comparisons are done in order to provide order of magnitude for the experimenters.

Keywords — Uncertainty Quantification, Bayesian inverse problems, Adaptive Metropolis with Covariance Matrix Adaptation, Neutronics, Complementarity time gates

NOMENCLATURE

Nuclear constants

α	Decreasing coefficient of the neutronic system
$\bar{\nu}$	Mean number of neutrons emitted by a fission event
$\bar{\nu}_S$	Mean number of neutrons emitted by a source event
λ_C	Capture rate by time unit
λ_F	Fission rate by time unit
D_{2S}	Diven factor of the source of order 2
D_2	Diven factor of the fission of order 2
D_{3S}	Diven factor of the source of order 3
D_3	Diven factor of the fission of order 3
f_ν	Probability the fission emits ν neutrons
$f_{\nu,S}$	Probability that source emits ν neutrons during a source event
p	Probability that a neutron causes a fission

Nuclear parameters

$\mathbf{p}$	Vector of the parameters of the system
ε_C	Capture efficiency
k_{eff}	Multiplication factor
S	Intensity of the source (neutron/units of time)

Measurements and model outputs

$\mathbf{M}$	Vector of the first three simple statistical moments, the model
$\widehat{\mathbf{M}}_T$	Vector of the first three simple empirical moments for a time gate T, the measures
T	Time gate (units of time)

Numerical Methods and associated terminology

CMA Covariance Matrix Adaptation

MAP Maximum A Posteriori

MC Monte-Carlo

MCMC Markov Chain Monte-Carlo

MCNP Monte Carlo N-Particle Transport Code, developed by Lawrence Livermore National Laboratory

MH Metropolis-Hastings

I. INTRODUCTION

We are interested in fissile matter detection and characterisation. We want to determine the fissile source with external measures. Times of neutron detection during an interval of measure provides the outputs.

We study here an inverse problems under limited data. The inverse problem is ill-posed, getting the entries of the model is challenging. This problem was studied by Hage and Cifarelli in their classic work [1, 2] where they provide the mean and the standard deviation of three parameters of the fissile matter.

To address this issue, we use Bayesian methods. We get the a posteriori distribution that provides the relative probability of the entries knowing the measures, our outputs [3]. This information is more elaborated than just a mean and a standard deviation, we also get credibility intervals. In order to sample the a posteriori distribution we will use a Markov Chain Monte-Carlo (MCMC) method: the Metropolis-Hastings (MH) algorithm. Previous work in the report of the Lawrence Livermore National Laboratory [4] settles a Bayesian method in multiplicity counting. More precisely, they use a Bayesian 'particle filter' in order to fit the detection interval distribution.

Since the a posteriori distribution is degenerate when the measures are extensive, we will use an Adaptive-Metropolis algorithm with Covariance Matrix Adaptation (CMA).

The paper is organized as follows. First, we introduce the neutron point model and expose the expressions of the simple moments of the neutrons count distribution [5].

Secondly, we will recall Bayes rules, present the requirements for the sampling and expose the given covariance for the measures. And we will also present the sampling of the a posteriori distribution, the discretisation with 3 parameters.

Thirdly, we will recall the results of the sampling with a benchmark. We will analyse the features of the sampled distribution with an explicit sampling and MCMC sampling.

Finally, we will expose a method in order to gain precision in the estimation of the best set of parameters for a given time of measurements, what could be interesting in the experiments. We will also discuss the efficiency of this method with regard to the duration of the time of measurements.

II. STOCHASTIC NEUTRONICS PROBLEM, FORWARD PROBLEM

In neutronics, the simplest model is the point model approximation. It was introduced by Feynman et al. [6] during the Manhattan Project.

Definition II.1. *Point model [7] The medium is infinite, homogeneous and isotropic. The neutrons are supposed point particles moving at the same speed. Moreover, we consider the neutron's life ends with a capture (with or without a detection) or a fission. These events are poissonian type. Neutrons are produced by fission and by the Poisson or compound Poisson type sources. A fission chain is modelled as a branching process.*

The model is governed by the following parameters.

II.A. Source

We model the source as a compound Poisson process with a strength S. The number of neutrons emitted by a source event is given by the probability distribution $f_{\nu,S}$ where ν goes from 0 to the maximum number of neutrons emitted by the source $\nu_{max,S}$. The mean number of neutrons emitted by one source event is $\bar{\nu}_S = \sum_{\nu=0}^{\nu_{max,S}} \nu f_{\nu,S}$.

From this, we can derive the nuclear constants of the source. The Diven factors of order 2 and 3 of the source probability distribution are $D_{2S} = \frac{\sum_\nu \nu(\nu-1) f_{\nu,S}}{\bar{\nu}_S^2}$ and $D_{3S} = \frac{\sum_\nu \nu(\nu-1)(\nu-2) f_{\nu,S}}{\bar{\nu}_S^3}$.

II.B. Fission

We define p as the probability that a neutron causes a fission (so $1-p$ is be the probability that a neutron be captured). The probability distribution of the number of neutrons produced by a fission is f_ν where ν goes from 0 to the maximum number of neutrons emitted by the fission ν_{max}, and $\bar{\nu} = \sum_{\nu=0}^{\nu_{max}} \nu f_\nu$ is the mean number of neutrons emitted by one fission event. When a fission occurs $\bar{\nu}$ neutrons are emitted on average. Then $k_{eff} = \bar{\nu} p$ is the mean number of children of a neutron. We will call it the multiplication factor [8].

In our case $0 < k_{eff} < 1$, which means sub-criticality. Under this assumption, the system will be called stationary when the probability distribution of the stochastic process of the number of neutrons present in the system is invariant under temporal shift. In mathematical terms, we will say that the system is stationary when the number of neutrons present in the system is ergodic (see [9] for more precise definition). A stationary system is the most important configurations for nuclear safety applications [10].

As for the source, we obtain the formulas of the Diven factors of the fission of order 2 and 3 $D_2 = \frac{\sum_\nu \nu(\nu-1)f_\nu}{\bar{\nu}^2}$, $D_3 = \frac{\sum_\nu \nu(\nu-1)(\nu-2)f_\nu}{\bar{\nu}^3}$. The fission rate is λ_F.

II.C. Capture

The neutron count is the action of detecting the neutron presence. The capture rate is λ_C. We define the capture efficiency ε_C as the probability that a captured neutron is detected. This efficiency is linked to the fission one ε_F by the equality $\varepsilon_F = \frac{\lambda_C \varepsilon_C}{\lambda_F}$. This is the ratio of the mean number of detections over the mean number of induced fissions.

II.D. Measurements

We get our outputs from a detector with Helium 3 [11]. Neutronicians choose this element because its cross-section is large, so the capture probability is high. Neutrons are absorbed in the detector with the reaction

$$^3_2\mathrm{He} +^0_1 \mathrm{n} \rightarrow^1_1 \mathrm{H} +^3_1 \mathrm{H} + 765\mathrm{keV}$$

then the proton emerging from the reaction causes an electric current. During a time interval of duration T_{meas}, each produced electric current are stored as instant of detection in a list file (see fig. 1). The detector is recording the detection times between t_0 and $t_{max} = t_0 + T_{meas}$. After a time T, the number of neutrons detected is counted. This number is stored as $N_{1,[0,T]}$, the first realisation of $N_{[0,T]}$, the counted neutrons during a time gate T. Then, we repeat this operation after each T to store the $(N_{l,[0,T]})_{l=1}^n$ where $n = \lfloor \frac{T_{meas}}{T} \rfloor$. Thus, we will be able to compute the empirical moments of the distribution $N_{[0,T]}$.

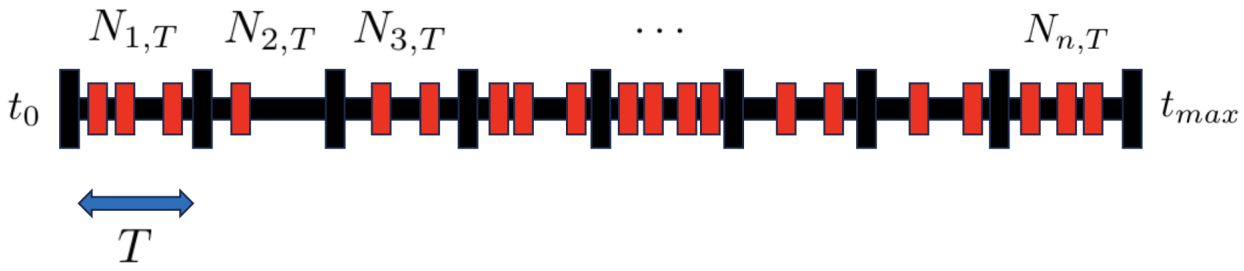

Fig. 1. A measurement between t_0 and $t_{max} = t_0 + T_{meas}$, with a time gate T

II.E. Forward model

Definition II.2. *Let $N_{[0,T]}$ be the random variable representing the neutron counts during T. The three first associated moments of this distribution are*

- $\mathbb{E}[N_{[0,T]}] :=$ *the first moment of the neutron counted during T distribution*
- $\mathbb{E}[N^2_{[0,T]}] :=$ *the second simple moment of the neutron counted during T distribution*
- $\mathbb{E}[N^3_{[0,T]}] :=$ *the third simple moment of the neutron counted during T distribution*

These are the outputs of our model.

Thus, for a time of measurements T_{meas}, we will estimate the three first moments of the distribution of $N_{[0,T]}$ using its empirical realisations $(N_{l,[0,T]})_{l=1}^n$ where $n = \lfloor \frac{T_{meas}}{T} \rfloor$

$$\begin{aligned}
\widehat{\mathbb{E}}[N_{[0,T]}] &= \frac{1}{n}\sum_{l=1}^{n} N_{l,[0,T]} \\
\widehat{\mathbb{E}}[N^2_{[0,T]}] &= \frac{1}{n}\sum_{l=1}^{n} N^2_{l,[0,T]} \\
\widehat{\mathbb{E}}[N^3_{[0,T]}] &= \frac{1}{n}\sum_{l=1}^{n} N^3_{l,[0,T]}
\end{aligned} \tag{1}$$

In the case of the point model the simple moments can be expressed as a function of the so-called Feynman moments $Y_2(T)$, $Y_3(T)$ [10].

Proposition II.3. *The first three simple moments of $N_{[0,T]}$ are of the form*

$$\begin{aligned}
\mathbb{E}[N_{[0,T]}] &= \bar{\nu}_S S \frac{\varepsilon_F k_{eff}}{(1-k_{eff})\bar{\nu}} T \\
\mathbb{E}[N^2_{[0,T]}] &= \mathbb{E}[N_{[0,T]}](1 + \mathbb{E}[N_{[0,T]}] + Y_2) \\
\mathbb{E}[N^3_{[0,T]}] &= \mathbb{E}[N_{[0,T]}](1 + 3Y_2 + Y_3) + 3\mathbb{E}[N_{[0,T]}]^2(1+Y_2) + \mathbb{E}[N_{[0,T]}]^3
\end{aligned} \tag{2}$$

where the Feynman moments are given by

$$
\begin{aligned}
Y_2(T) &= \frac{\varepsilon_F D_2 k_{eff}}{(k_{eff}-1)^2}\left(1-\frac{k_{eff}-1}{k_{eff}}\frac{\bar{\nu}_S D_{2S}}{\bar{\nu} D_2}\right)\left(1-\frac{1-e^{-\alpha T}}{\alpha T}\right)\\
Y_3(T) &= 3\left(\frac{\varepsilon_F D_2 k_{eff}}{-(1-k_{eff})^2}\right)^2\left(1-\frac{k_{eff}-1}{k_{eff}}\frac{\bar{\nu}_S D_{2S}}{\bar{\nu} D_2}\right)\left(1+e^{-\alpha T}-2\frac{1-e^{-\alpha T}}{\alpha T}\right)\\
&\quad-\frac{\varepsilon_F D_3 k_{eff}^3}{(k_{eff}-1)^3}\left(1-\frac{k_{eff}-1}{k_{eff}}\frac{\bar{\nu}_S^2 D_{3S}}{\bar{\nu}^2 D_3}\right)\left(1-\frac{3-4e^{-\alpha T}+2e^{-2\alpha T}}{\alpha T}\right)
\end{aligned}
\tag{3}
$$

where $\alpha = \lambda_C + \lambda_F(1-\bar{\nu})$.

A proof of this result can be found in [9] in the part 1.6.3 using $\rho = \frac{k_{eff}-1}{k_{eff}}$. And so we obtain

Proposition II.4. *When* $T >> \frac{1}{\alpha}$*, the asymptotical expressions of the simple moments are*

$$
\begin{aligned}
\mathbb{E}[N_{[0,T]}] &= \bar{\nu}_S S \frac{\varepsilon_F k_{eff}}{(1-k_{eff})\bar{\nu}} T\\
\mathbb{E}[N^2_{[0,T],\infty}] &= \mathbb{E}[N_{[0,T]}](1+\mathbb{E}[N_{[0,T]}]+Y_{2,\infty})\\
\mathbb{E}[N^3_{[0,T],\infty}] &= \mathbb{E}[N_{[0,T]}](1+3Y_{2,\infty}+Y_{3,\infty})+3\mathbb{E}[N_{[0,T]}]^2(1+Y_{2,\infty})+\mathbb{E}[N_{[0,T]}]^3
\end{aligned}
\tag{4}
$$

where the asymptotical expressions of the Feynman moment are

$$
\begin{aligned}
Y_{2,\infty}(T) &= \frac{\varepsilon_F D_2 k_{eff}}{(k_{eff}-1)^2}\left(1-\frac{k_{eff}-1}{k_{eff}}\frac{\bar{\nu}_S D_{2S}}{\bar{\nu} D_2}\right)\\
Y_{3,\infty}(T) &= 3\left(\frac{\varepsilon_F D_2 k_{eff}}{-(1-k_{eff})^2}\right)^2\left(1-\frac{k_{eff}-1}{k_{eff}}\frac{\bar{\nu}_S D_{2S}}{\bar{\nu} D_2}\right)\\
&\quad-\frac{\varepsilon_F D_3 k_{eff}^3}{(k_{eff}-1)^3}\left(1-\frac{k_{eff}-1}{k_{eff}}\frac{\bar{\nu}_S^2 D_{3S}}{\bar{\nu}^2 D_3}\right)
\end{aligned}
\tag{5}
$$

This is a direct consequence of the previous proposition. So, when $T >> \frac{1}{\alpha}$, the simple moments behave as $\mathbb{E}[N_{[0,T]}]$ to the power of the order of the considered moment. These last expression of the moments show there are two different regimes we can consider :

- when $T << \frac{1}{\alpha}$, so the expression of the simple moments contains polynomials of order $\frac{1-e^{-\alpha T}}{\alpha T}$ or $\frac{1-e^{-2\alpha T}}{\alpha T}$;
- when $T >> \frac{1}{\alpha}$, so the expression of the simple moments are polynomials of $\mathbb{E}[N_{[0,T]}]$ to the power the order of the considered moment.

Then, we can deduce the asymptotic behaviour of the three first simple moments in the stationary regime, when $T >> \frac{1}{\alpha}$, and compare it to the transitionary regime, $T << \frac{1}{\alpha}$. This will be interesting for the last method introduced.

Our forward model is

$$\begin{array}{rcl} \mathbf{M} : \mathbb{R}^3 & \rightarrow & \mathbb{R}^3 \\ \mathbf{p} & \mapsto & \mathbf{M}(\mathbf{p}, T) \end{array} \tag{6}$$

where $\mathbf{p} = (\varepsilon_C, k_{eff}, S)$ and $\mathbf{M}_j(\mathbf{p}) = \mathbb{E}[N^j_{[0,T]}]$ for $j \in [\![1; 3]\!]$. We will denote the associated estimation $\widehat{\mathbf{M}}_T$.

It is important to keep in mind that the point model and our forward model are simplistic. In real application, the dependency on the time gate is more complex. Moreover, dead-time effects should be taken into account, see [12] for further details.

III. THE "COUNTING" CODE, A MC CODE IN THE POINT MODEL APPROXIMATION

In the point model approximation, we established the Monte-Carlo (MC) code 1, which is a kinetic Monte-Carlo code (a good introduction can be found in [13]).

Algorithm 1: Couting code, the Monte-Carlo code in the point model approximation, generating a TimeList file

$\lambda_{C,loc}$;
$\lambda_{F,loc}$;
S;
for $i = 1, \textit{Number of realizations}$ **do**
  $t = 0$;
  $X_t = 1$;
  $\lambda_C = X_t \lambda_{C,loc}$;
  $\lambda_F = X_t \lambda_{F,loc}$;
  $L = S + \lambda_C + \lambda_F$;
  while $t < t_{max}$ **do**
    $u \sim \mathcal{U}[0, 1]$;
    $dt = -\frac{log(u)}{L}$;
    CALL Simulations of either the source, the fission, the capture (with or without a detection) (algo 2);
    $\lambda_C = X_t \lambda_{C,loc}$;
    $\lambda_F = X_t \lambda_{F,loc}$;
    $L = S + \lambda_C + \lambda_F$;
    Storage of the values of X_t and t for post-treatment;
    $t = t + dt$;
  end
end

Algorithm 2: Simulation of the events: source, fission or capture (with or without a detection)

$invl = \frac{1}{L}$;
$p_S = S * invl$;
$p_C = \lambda_C * invl$;
$p_F = \lambda_F * invl$;
$u \sim \mathcal{U}[0,1]$;
$process\_index = \mathbf{1}_{[0,p_S]}(u) + 2\mathbf{1}_{[p_S,p_S+p_C]}(u) + 3\mathbf{1}_{[p_S+p_C,1]}(u)$;
if *process_index == 1 (Source)* **then**
    % Computation of the random number of neutrons emitted by the source;
    Call number_of_emitted_neutrons_by_the_sources(nu);
    $X_t = X_t + nu$;
else if *process_index == 2 (Capture)* **then**
    $X_t = X_t - 1$;
    $u \sim \mathcal{U}[0,1]$;
    $x\_compt = \mathbf{1}_{[0,\varepsilon_C]}(u) + 2\mathbf{1}_{[\varepsilon_C,1]}(u)$;
    if $x\_compt == 1$ **then**
        Storage of the time of detection;
        Number of detections = number of detections+1;
else if *process_index == 3 (Induced fission)* **then**
    % Computation of the random number of neutrons emitted by the fission;
    Call number_of_emitted_neutronsby_the_fission(ne);
    $X_t = X_t + ne - 1$;

The algorithm 1 allows verifying the analytical formulas of the different moments by the Monte-Carlo method. More precisely, this code provides the detection times of the counts and the number of neutrons present in the system by the Monte-Carlo method, and thus a Time List file that can be analysed (in the presence or absence of a source). After processing the Time List file, we implemented the explicit Euler method for each of the quantities of interest and verified the analytical expressions with it.

Another part of the code provides the processing of the Time List file and the analytical and explicit Euler checks (see 2.4 of [9]). It also provides detailed statistical analysis results, particularly for the direct problem.

IV. BAYESIAN INVERSE PROBLEM

An inverse problem is defined as [3]: knowing some outputs $\mathbf{y}_{out}$, we want to find the parameters $\mathbf{p}$ of a given model $\mathbf{M}'$ where

$$\mathbf{y}_{out} = \mathbf{M}'(\mathbf{p}) \tag{7}$$

IV.A. Bayes principle

We have the outputs $\mathbf{y}_{out} = \widehat{\mathbf{M}}_T$ which are the estimated moments of $N_{[0,T]}$. Bayes theorem [14] states

$$\underset{a\ posteriori\ distribution}{\mathbb{P}(\mathbf{p}|\widehat{\mathbf{M}}_T)} \propto \underset{likelihood}{\mathbb{P}(\widehat{\mathbf{M}}_T|\mathbf{p})} \underset{a\ priori\ distribution}{\mathbb{P}(\mathbf{p})} \tag{8}$$

where the likelihood and the a priori distribution are as follows

1. Thanks to the Central Limit Theorem, given the parameter $\mathbf{p}$ the measures are Gaussian with mean $\mathbf{M}(\mathbf{p},T)$ and covariance $\frac{1}{n}\mathbf{Cov}(\mathbf{p},T)$ where $\mathbf{M}$ refers to the expression of the exact simple moments of the distribution of $N_{[0,T]}$, $\mathbf{Cov}(\mathbf{p},T)$ the covariance matrix of the three first simple moments, n the number of realizations.

   As defined in the figure 1, the realizations of $N_{[0,T]}$ are dependent. In this case, the Central Limit Theorem does not apply rigorously. In the experiments, it is reasonable to consider approximately true.

   This gives explicitly

   $$\mathbb{P}(\widehat{\mathbf{M}}_T|\mathbf{p}) \propto \frac{1}{\sqrt{det(\frac{1}{n}\mathbf{Cov}(\mathbf{p},T))}} e^{-\frac{1}{2}\ {}^t(\widehat{\mathbf{M}}_T-\mathbf{M}(\mathbf{p},T))\mathbf{Cov}(\mathbf{p},T)^{-1}(\widehat{\mathbf{M}}_T-\mathbf{M}(\mathbf{p},T))n} \tag{9}$$

   which is the expression of the likelihood up to a multiplicative constant.

   The computation of $\mathbf{Cov}(\mathbf{p},T)$ needs the expression of the simple moments up to the order 6, and this is too complex to be computed analytically. So we will use the empirical covariance matrix $\widehat{\mathbf{Cov}}_T$ whose coefficients at the i-th row and j-th column are given by

   $$\widehat{\mathbf{Cov}}_{T,i,j} = \frac{1}{n}\sum_{l=0}^{n} N^i_{l,[0,T]} N^j_{l,[0,T]} - \left(\frac{1}{n}\sum_{l=0}^{n} N^i_{l,[0,T]}\right)\left(\frac{1}{n}\sum_{l=0}^{n} N^j_{l,[0,T]}\right) \text{ for } i,j = 1,2,3. \tag{10}$$

   The corresponding likelihood is

   $$\tilde{\mathbb{P}}(\widehat{\mathbf{M}}_T|\mathbf{p}) \propto \frac{1}{\sqrt{det(\frac{1}{n}\widehat{\mathbf{Cov}}_T)}} e^{-\frac{1}{2}\ {}^t(\widehat{\mathbf{M}}_T-\mathbf{M}(\mathbf{p},T))\widehat{\mathbf{Cov}}_T^{-1}(\widehat{\mathbf{M}}_T-\mathbf{M}(\mathbf{p},T))n} \tag{11}$$

2. The a priori distribution is assumed to be uniform on $[\varepsilon_{C,min},\varepsilon_{C,max}] \times [k_{min},k_{max}] \times [S_{min},S_{max}]$.

Our goal is to sample the a posteriori distribution 8. We will use two different methods: a discrete sampling with a regular mesh and Adaptive Metropolis with Covariance Matrix Adaptation.

IV.B. Explicit sampling of the a posteriori distribution

A simple way to obtain the explicit sampling of the a posteriori distribution is to use a regular mesh of the domain $[\varepsilon_{C,min}, \varepsilon_{C,max}] \times [k_{min}, k_{max}] \times [S_{min}, S_{max}]$ and compute the a posteriori distribution on each point of the mesh. The computations were done with N_e points in each directions. The overall number of evaluations of the forward model 6 is therefore N_e^3. We also compute the moments in order to have some quantitative information: mean, variance, expectation to be compared with MCMC results.

Remark IV.1. *By 8 the computation of the likelihood is true up to a multiplicative constant.*

IV.C. MCMC sampling of the a posteriori distribution

The principle of the method is to build a Markov chain that has the target distribution, denoted π, as its stationary distribution. Hence one can obtain a sample of the target distribution by sampling and recording states from the chain. Various algorithms exist for constructing such Markov chains, including the Metropolis-Hastings (MH) algorithm. The states of the MH chain are produced iteratively. At each iteration, the algorithm choose a random proposal according to some instrumental distribution that may depend on the current sample value. The proposal is the candidate for the next sample value and it is either accepted (in which case the proposal value is used in the next iteration) or rejected (in which case the proposal value is discarded, and the current value is used in the next iteration) with some probability. The probability of acceptance is determined by comparing the values of the target density at the current and proposal values so as to ensure that the MH chain has the target distribution as its stationary distribution.

We have implemented the Metropolis-Algorithm with Covariance Matrix Adaptation of [15] and [16]. As previously we consider the parameter $\mathbf{p}$ and we consider the same parameter bounds $p_{1,min} = \varepsilon_{C,min},\ p_{1,max} = \varepsilon_{C,max},\ p_{2,min} = k_{min},\ p_{2,max} = k_{max},\ p_{3,min} = S_{min},\ p_{3,max} = S_{max}$

The adaptation uses the Covariance Matrix of the all the points proposed by the instrumental law and accepted by the rejection procedure in order to accept more.

We first initiate

- The empirical acceptance x_{rate}.
- The initial scale factor of the instrumental law $frac$
- The target acceptance rate x_{obj}
- The frequency of update of the scale factor $N_{MC,1}$

- The burn-in phase duration N_{bp}
- The initial parameter $\mathbf{p}_0$ is chosen with the uniform distribution over $\bigotimes_{k=1}^{3}[p_{k,min}, p_{k,max}]$

Iteration $i \to i+1$

1. During $i \leq N_{bp}$, we use as instrumental law

$$\mathbf{q}_{i+1} \sim \mathcal{N}(\mathbf{p}_i, frac^2\mathbf{C}_{bi}) \tag{12}$$

   where $\mathbf{q}_{i+1}$ the proposal, $\mathbf{p}_i$ the last accepted point, $\mathbf{C}_{bi} = diag(((p_{k,max} - p_{k,min})^2)_{k=1}^3)$.

2. After the burnin we use the instrumental law as in algorithm 4 of [15]

$$\mathbf{q}_{i+1} \sim \mathcal{N}(\mathbf{p}_i, frac^2\mathbf{C}_i) \tag{13}$$

   where $\mathbf{C}_i$ is defined by 16.

3. Finally, we compute the acceptance rate α_{acc} using the likelihood ratio of the proposal and the previous accepted point

$$\alpha_{acc}(\mathbf{q}_{i+1}, \mathbf{p}_i) = min(1, \frac{\pi(\mathbf{q}_{i+1})}{\pi(\mathbf{p}_i)}) \tag{14}$$

4. The acceptance-rejection criterion

$$\begin{aligned} &u \sim \mathcal{U}([0,1]) \\ &\text{If } \; u \leq \alpha_{acc}(\mathbf{q}_{i+1}, \mathbf{p}_i) \text{ then } \; \mathbf{q}_{i+1} \text{ is accepted: } \mathbf{p}_{i+1} = \mathbf{q}_{i+1} \text{ otherwise } \mathbf{p}_{i+1} = \mathbf{p}_i \end{aligned} \tag{15}$$

   is applied

5. We update the scale factor when $i \equiv 0(\mod N_{MC,1})$. The scale factor $frac$

$$\begin{aligned} frac &= frac\ exp(x_{rate} - x_{obj}) \\ x_{rate} &= \frac{\text{Number of acceptations}}{\text{Number of iterations}} \end{aligned}$$

This is an algorithm with global scaling and vanishing adaptation, so that the ergodicity of the algorithm is achieved. Here the vanishing factor is $\gamma_i = \frac{1}{i}$, it must be chosen such that $\sum_i \gamma_i = +\infty$ (explained in [15]), more explanation in the next paragraphs.

The covariance matrix and the mean of the proposal are updated as in [17]

$$\begin{aligned}\bar{\mathbf{p}}_{i+1} &= (1-\gamma_{i+1})\bar{\mathbf{p}}_i + \gamma_{i+1}\mathbf{p}_i \\ \mathbf{C}_{i+1} &= (1-\gamma_{i+1})\mathbf{C}_i + \gamma_{i+1}(\mathbf{p}_i - \bar{\mathbf{p}}_i)^T(\mathbf{p}_i - \bar{\mathbf{p}}_i)\end{aligned} \tag{16}$$

The work of [18] provides an analysis of the Metropolis-Hastings algorithm regarding the acceptance rate. Then we choose $frac = \frac{2,4}{\sqrt{d}}$ where $d = dim(\mathbf{p})$ as suggested in [18].

The target $x_{obj} = 0.234$ is chosen thanks to [18].

We will define a probability distribution as degenerate when it is supported on a manifold of lower dimension.

Here the a posteriori distribution support can be degenerate. As example, when the time of measurements is 3600s and $k_{eff} = 0.95$, the support of the a posteriori distribution is very small (see part V), thus, we will mention it as very degenerate. When we dispose of more than 3 parameters, two things arise : the computational cost of the explicit sampling is too high, and also, the MCMC method must find the manifold where the a posteriori distribution is supported.

So the use of $\mathbf{C}$ and the global factor adaptation allows to sample well the distribution, even if highly degenerated.

As the target distribution is very degenerate, it is difficult to sample it with a classical Metropolis-Hastings algorithm. The best algorithm we can have is an algorithm whose exploration law is equal to our target distribution. To sample this target distribution, we use a vanishing factor γ_i (here $\gamma_i = \frac{1}{i}$) so that the exploration distribution coincides with the target distribution. The vanishing factor γ_i will tend to zero so that the exploration law fits the target distribution well.

We have seen that the algorithm works well in the cases studied, but the more parameters we take into account, the more difficult the algorithm becomes. The MCMC methods provide a sampling of the distribution of the parameters $\mathbf{p}$ given the outputs of our system $\widehat{\mathbf{M}}_T$.

We give the details in the pseudo-code of our algorithm in 3, 4 and 5. In practice, the time of computation of the algorithm is around 10min. This is an asset for real time application.

In the following, we present the results of the calculation of the posterior distribution obtained on test cases. Two numerical methods are used. The first one, the explicit method, is deterministic and based on the discretisation of the calculated distribution on a regular grid. In the second method, the distribution is sampled using an MCMC algorithm. The explicit method becomes very expensive when the parameter space is large. It is used for verification of the MCMC method when the number of parameters is less than or equal to three. The advantage of the MCMC method is that it can be used at a reasonable cost when the number of parameters is greater than

Algorithm 3: Comparison MCMC with CMA sampling and explicit sampling (see IV.C)

Initialisations;
Dimension of $\mathbf{p} = 3$;
Number of time gates $= 2$;
$\mathbf{p}^*$ and $\mathbf{p}_{min}, \mathbf{p}_{max}$;
T_1, T_2 and T_{meas};
Outputs and covariance matrix for T_1 and T_2;
Nuclear constants ν, D_2, D_3 and ν_S, D_{2S}, D_{3S};
Printing the simple moments, the covariance matrix and correlation matrix;
Inversion of the covariance matrix, printing its determinant;
Print the covariance matrix times its inverse;
Number of MCMC iterations $= 5 \times 10^7$;
Number of points for the 1D and 2D histograms $= 100$;
MCMC with CMA sampling;
Number of points for the 1D and 2D histograms;
Explicit sampling;
Printing the mean, standard deviation, 1D and 2D marginals

three.

V. TEST-CASES, NUMERICAL APPLICATION

The a posteriori distribution can be degenerate, a parameter study of the a posteriori distribution was already established in [19]. To summarize the results of this study, we observed that when k_{eff} is close to 1 and the time of measurements T_{meas} is of order 3600s the a posteriori distribution is very degenerate. So, the use of MCMC methods with CMA is required.

VI. CONSIDERING TWO COMPLEMENTARY REGIMES

As we can observe in the expression of the simple moments of $N_{[0,T]}$ in proposition II.3 and II.4, their expression have two different behaviours when the regime is transitionary, $T << \frac{1}{\alpha}$, or stationary, $T >> \frac{1}{\alpha}$ where α is the inverse fission chain evolution timescale [20]. Moreover, by considering these time gates, we observe the support of the a posteriori distribution can be different. This will be confirmed by the numerical experiments. Regarding the measurements, we still record the detection times between t_0 and $t_{max} = t_0 + T_{meas}$ and do a first measurement considering T_1 and then do a separate measure T_2. Thus, the measurements for T_1 and T_2 are independents.

Dead-time effects in the considered detectors are of order μs. The time gate T_1 is $0.5ms$. In the following examples, $\mathbb{E}[N_{[0,T_1]}] \approx 0.14$ then the average number of counts is $\frac{\mathbb{E}[N_{[0,T_1]}]}{T_1} \approx$

Algorithm 4: MCMC with CMA sampling algorithm (see IV.C)

Initialisations
Random seed;
$N_{bp} = max(\frac{\text{Number of MCMC iterations}}{10}, 1)$;
$\mathbf{p}_0$;
Computation of $\mathbf{M}(\mathbf{p}_0)$;
$oldlike = log(\pi(\mathbf{p}_0))$;
$x_{rate} = 1$, $frac = 0.1$, $N_{MC,1} = max(\frac{N_{MC}}{10000}, 1)$, $x_{obj} = 0.234$;
for $i = 1, Number\ of\ MCMC\ iterations$ **do**
    $\mathbf{p}_i = \mathbf{p}_{i-1}$;
    if $i \leq N_{bp}$ **then**
        if $i \equiv 0(\mod N_{bp})$ **then**
            $xx = exp(x_{rate} - x_{obj})$;
            $frac = max(frac \times xx, 10^{-3})$;
            $frac = min(frac, 1)$;
        $\mathbf{q}_{i+1} \sim \mathcal{N}(\mathbf{p}_i, frac^2\mathbf{C}_{bi})$ using gasDev routine;
    else
        if $i \equiv 0(\mod N_{bp})$ **then**
            Updating $\mathbf{p}_i$ and $\mathbf{C}_i$ as in eq. 16 and (adding $10^{-9}\mathbf{Id}$, using Cholesky factorisation for numerical stability);
            $xx = exp(x_{rate} - x_{obj})$;
            $frac = max(frac \times xx, 10^{-3})$;
            $frac = min(frac, 1)$;
        $\mathbf{q}_{i+1} \sim \mathcal{N}(\mathbf{p}_i, frac^2\mathbf{C}_i)$ using gasDev;
    end
    Next iteration if $\mathbf{q}_{i+1}$ outside of boundaries;
    Computation of $\mathbf{M}(\mathbf{q}_{i+1})$ and $newlike = log(\pi(\mathbf{q}_{i+1}))$;
    $dlike = newlike - oldlike$;
    $dlike = min(dlike, 200)$;
    $dlike = max(dlike, -200)$;
    $ratio = exp(dlike)$;
    $u \sim \mathcal{U}(0, 1)$;
    if $u \leq ratio$ **then**
        Number of acceptation +=1;
        $\mathbf{p}_i = \mathbf{q}_{i+1}$;
        $oldlike = newlike$;
end
Print overall x_{rate};
Create 1D and 2D histograms;

Algorithm 5: Explicit sampling algorithm (see IV.C)

Computations of π on $\bigotimes_{k=1}^{3}[p_{k,min}, p_{k,max}]$ with N_e points in each direction;
Create 1D and 2D histograms;

$0.28 \times 10^{-3} counts.s^{-1}$ which is less than $100 counts.s^{-1}$. Thus, the dead-time effects of the detector can be neglected.

As we observed in a previous paper [19], the support of the a posteriori distribution is wide when the time measurement is 3600s and

$$\mathbf{p}^* = \begin{pmatrix} S \\ k_{eff} \\ \varepsilon_C \end{pmatrix} = \begin{pmatrix} 70\ ms^{-1} \\ 0.5 \\ 0.25 \times 10^{-2} \end{pmatrix} \tag{17}$$

So we will consider two time gates in this case.

In the upcoming experiments, we will refer to MC outputs when the MCMC method use the likelihood in eq. 9 where $\mathbf{y}_{out} = \widehat{\mathbf{M}}_T$ and the associated covariance matrix $\widehat{\mathbf{Cov}}_T$ are computed from eq. 1 and 10 using the MC code 1. In the same way, we will refer to exact outputs when $\mathbf{y}_{out} = \mathbf{M}(\mathbf{p}^*, T)$ and the associated covariance matrix $\mathbf{Cov}(\mathbf{p}, T)$ are used in the likelihood.

Here, we refer to the absolute error

$$|QoI_{exact} - QoI_{MC}|, \tag{18}$$

as the difference between the exact value of the quantity of interest QoI_{exact} and the value estimated by the MC code QoI_{MC}.

VI.A. A posteriori distribution of $(k_{eff}, \varepsilon_C, S)$ given the three first moments of $N_{[0,T_1]}$, $N_{[0,T_2]}$ where $T_1 = \frac{1}{\alpha}$, $T_2 = \frac{10}{\alpha}$ and $k_{eff} = 0.5$

VI.A.1. For a time of measurement 3600s with exact outputs

In the third chapter of the thesis [9], we have obtained the results for the two distinct regimes $T << \frac{1}{\alpha}$ and $T >> \frac{1}{\alpha}$. We will consider the product of the a posteriori distribution of these two experiments for $N_{bp} = 5 \times 10^7$, and for the explicit sampling, we considered 1000 points on each direction.

The outputs are

$$\mathbf{y}_{out} = \begin{pmatrix} \mathbf{M}(\mathbf{p}^*, T_1) \\ \mathbf{M}(\mathbf{p}^*, T_2) \end{pmatrix} = \begin{pmatrix} 0.14043 \\ 0.16058 \\ 0.20382 \\ 1.4043 \\ 3.3868 \\ 10.165 \end{pmatrix} \tag{19}$$

Since the measurements associated with the two time gates are not correlated, the covariance matrix is

$$\begin{pmatrix} \mathbf{Cov}(\mathbf{p}^*, T_1) & (0) \\ (0) & \mathbf{Cov}(\mathbf{p}^*, T_2) \end{pmatrix} =$$

$$\begin{pmatrix} 0.19563 \times 10^{-7} & 0.25177 \times 10^{-7} & 0.37637 \times 10^{-7} & & & \\ 0.25177 \times 10^{-7} & 0.38033 \times 10^{-7} & 0.67808 \times 10^{-7} & & (0) & \\ 0.37637 \times 10^{-7} & 0.67808 \times 10^{-7} & 0.14152 \times 10^{-6} & & & \\ & & & 0.19649 \times 10^{-5} & 0.75127 \times 10^{-5} & 0.30420 \times 10^{-4} \\ & (0) & & 0.75127 \times 10^{-5} & 0.34313 \times 10^{-4} & 0.15688 \times 10^{-3} \\ & & & 0.30420 \times 10^{-4} & 0.15688 \times 10^{-3} & 0.78938 \times 10^{-3} \end{pmatrix} \tag{20}$$

First, we observe the 1D marginal distribution of each parameter. We can see that each marginal distribution corresponds to explicit sampling and MCMC sampling. The statistical noise is smaller than the aliasing noise.

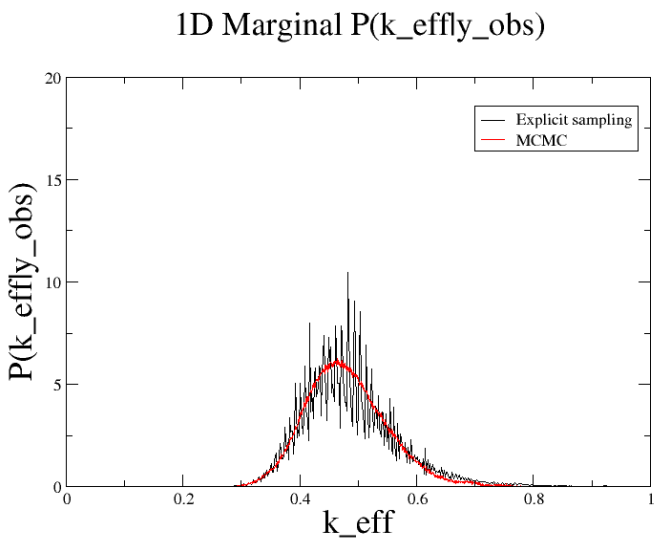

Fig. 2. Marginal distribution of k_{eff} with explicit sampling (black) and MCMC sampling (red)

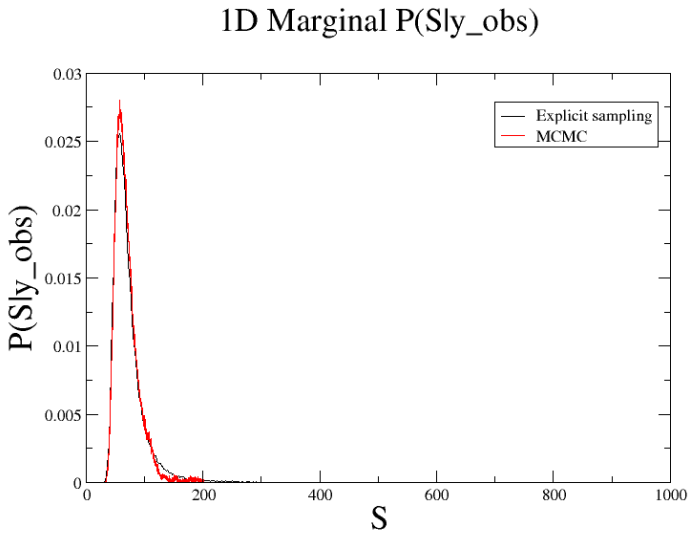

Fig. 3. Marginal distribution of S with explicit sampling (black) and MCMC sampling (red)

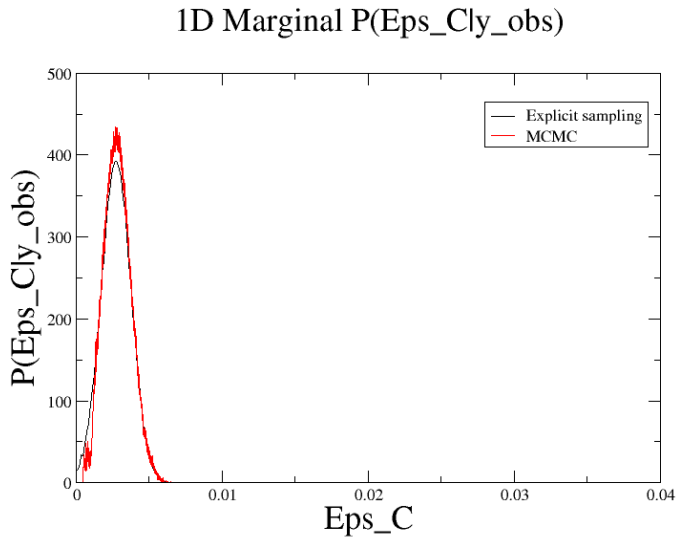

Fig. 4. Marginal distribution of ε_C with explicit sampling (black) and MCMC sampling (red)

The tables I and II shows the mean and standard deviation for the MCMC sampling and the explicit. The standard deviations are smaller for the MCMC method than for the explicit sampling. However, the estimated values are better for k_{eff} and ε_C.

Based on the smaller standard deviations, we draw the following conclusions: for $T_1 = \frac{1}{\alpha}$ and $T_2 = \frac{10}{\alpha}$, MCMC sampling is better than explicit sampling. Further reading of the section 3.2.3.

	$\mathbb{E}[k_{eff}\|\mathbf{y}_{out}]$	$\mathbb{E}[S\|\mathbf{y}_{out}]$	$\mathbb{E}[\varepsilon_C\|\mathbf{y}_{out}]$
MCMC	0.48026	69.441 ms^{-1}	0.28338×10^{-2}
Explicit	0.48723	74.019 ms^{-1}	0.27424×10^{-2}

TABLE I
The mean for the MCMC sampling and the explicit sampling with T_1 and T_2 for 3600s and exact outputs

	$\sqrt{\mathbb{E}[(k_{eff} - \mathbb{E}[k_{eff}\|\mathbf{y}_{out}])^2\|\mathbf{y}_{out}]}$	$\sqrt{\mathbb{E}[(S - \mathbb{E}[S\|\mathbf{y}_{out}])^2\|\mathbf{y}_{out}]}$	$\sqrt{\mathbb{E}[(\varepsilon_C - \mathbb{E}[\varepsilon_C\|\mathbf{y}_{out}])^2\|\mathbf{y}_{out}]}$
MCMC	0.69752×10^{-1}	20.656 ms^{-1}	0.92588×10^{-3}
Explicit	0.82327×10^{-1}	40.178 ms^{-1}	0.10101×10^{-2}

TABLE II
The standard deviation for the MCMC sampling and the explicit sampling with T_1 and T_2 for 3600s and exact outputs

of the thesis [9] show that the standard deviation of the estimation of $\mathbf{p}$ are smaller than with T_1 or T_2.

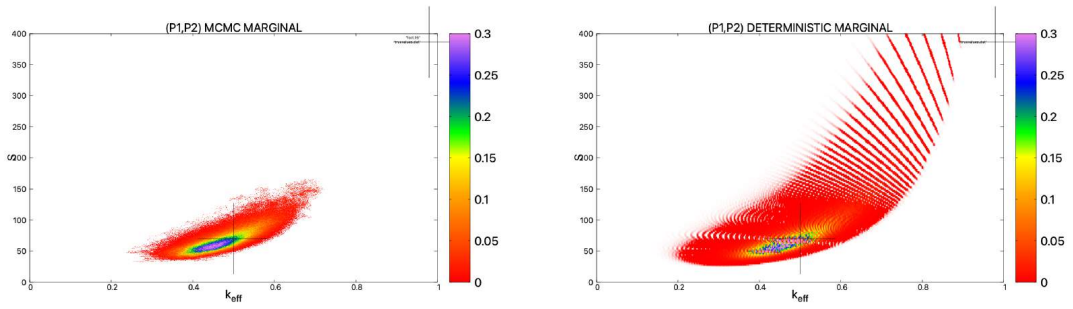

(a) MCMC sampling (b) Explicit sampling

Fig. 5. Marginal distribution of k_{eff} and S

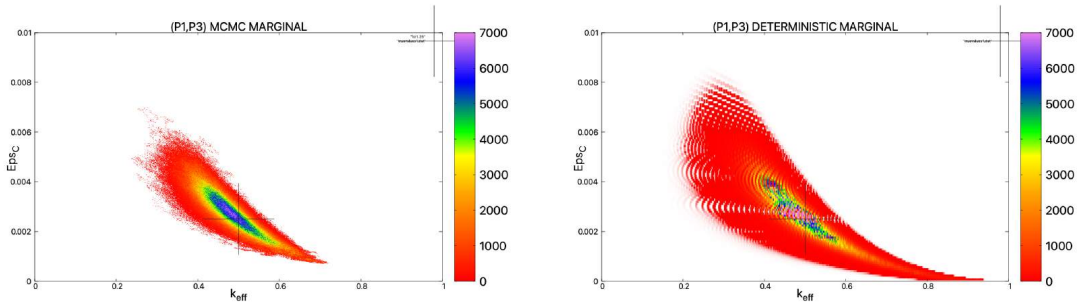

(a) MCMC sampling (b) Explicit sampling

Fig. 6. Marginal distribution of k_{eff} and ε_C

We provide the fig. 7 and 8 in order to have a better comparison of the marginals for $T_1 = \frac{1}{\alpha}$, $T_2 = \frac{10}{\alpha}$ and (T_1, T_2).

The results of the MCMC sampling using (T_1, T_2) in subfig. (c) of fig. 7 and 8 are as follows.

With three equations, such as the equations of the first three simple moments of $N_{[0,T]}$, we can expect to find at most three parameters. When there are more than three parameters to estimate, we have to find a way to calculate more. Taking into account the Feynman moment of order 4 could have been considered but only when ε_C is high. We recall that the equations of $\mathbb{E}[N_{[0,T]}]$, $Y_2(T)$, $Y_3(T)$ depend on T. So here we will consider two observation regimes: $T << \frac{1}{\alpha}$ and $T >> \frac{1}{\alpha}$. Both regimes can be taken into account in order to cross-check the information, thus obtaining a better estimate of $\mathbf{p}|\mathbf{y}_{out}$. We will explain this in the following paragraphs.

Considering the 1D marginal distribution for k_{eff} of the MCMC sampling with (T_1, T_2), we know that the mean of this 1D marginal distribution have a mean of 0.48026 and a standard deviation of 0.69752×10^{-1} (where the mean is 0.47937 and the standard deviation is 0.84720×10^{-1} for T_1, and 0.46896 and 0.84000×10^{-1} for T_2). So regarding the MCMC sampling, the 1D marginal distribution of k_{eff} with (T_1, T_2) is a better estimation of $k^*_{eff} = 0.5$ than with T_1 or T_2 alone because the mean is closer to the real value and the standard deviation is smaller than for the two other time gates.

The same kind of result can be observed for S and ε_C. So, regarding the 1D marginal distribution, the use of (T_1, T_2) is more recommended than T_1 or T_2 alone.

For the 2D marginal distribution of k_{eff} and S, we notice that the mode of the a posteriori distribution has a higher probability in figure (c) than in figures (a) and (b). Thus, the marginal distribution over k_{eff} and S is more concentrated, and thus gives a better estimate of $\mathbf{p}^*$.

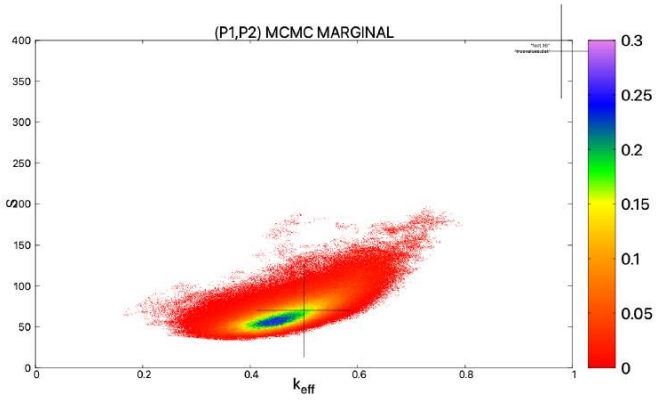

(a) $T_1 = \frac{1}{\alpha}$

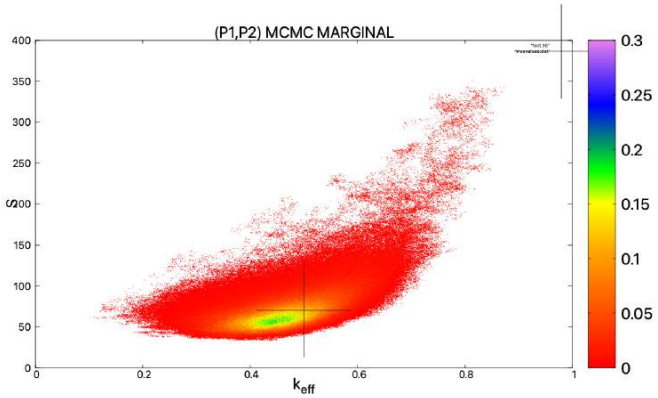

(b) $T_2 = \frac{10}{\alpha}$

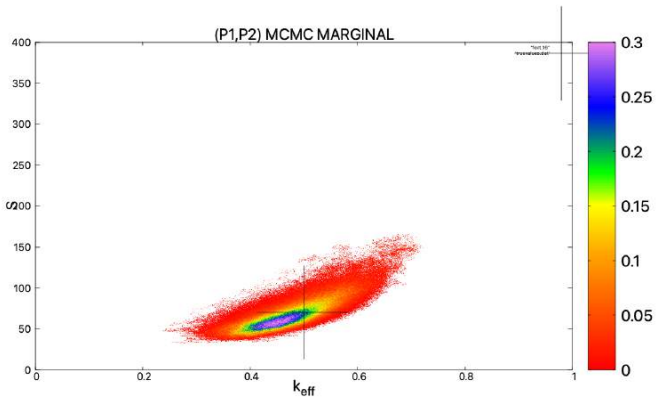

(c) (T_1, T_2)

Fig. 7. Marginal distribution of k_{eff} and S for T_1, T_2 and (T_1, T_2) with MCMC sampling

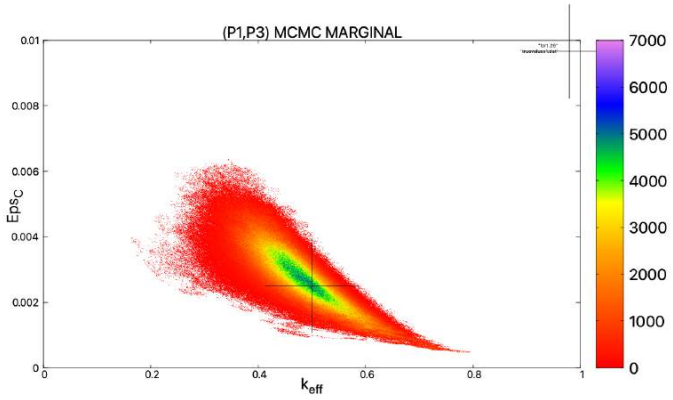

(a) $T_1 = \frac{1}{\alpha}$

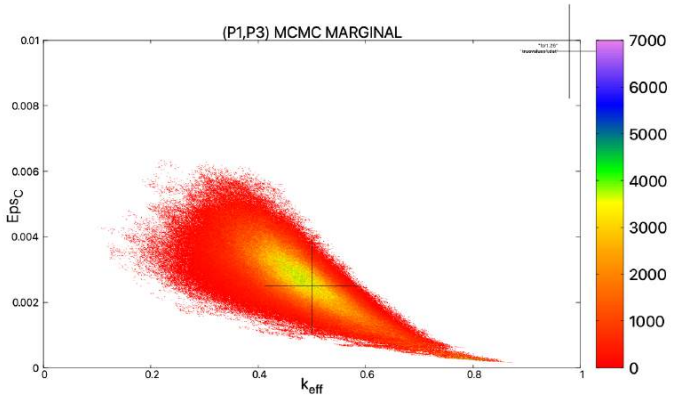

(b) $T_2 = \frac{10}{\alpha}$

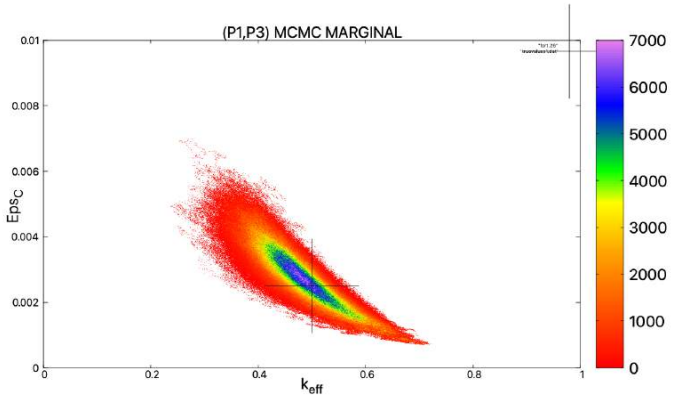

(c) (T_1, T_2)

Fig. 8. Marginal distribution of k_{eff} and ε_C for T_1, T_2 and (T_1, T_2) with MCMC sampling

In the same way, we can analyse the marginal distribution of k_{eff} and ε_C, we also notice that the mode is more likely than the two previous figures.

We can conclude that considering two time gates (T_1, T_2), in this case, enables to gain information through the marginal distributions. As the figures 2, 3, 4 and 5 in [19] shows, the a posteriori distribution is wider when k_{eff} is low and the time of measurements T_{meas} is low, so considering the two regimes when $T >> \frac{1}{\alpha}$ and $T << \frac{1}{\alpha}$ provide more information in these cases rather than when k_{eff} is high and the time of measurements T_{meas} is high. In these last cases, considering $T >> \frac{1}{\alpha}$ and $T << \frac{1}{\alpha}$ provide no significant information gain.

As the behaviour of the simple moments depends on the regime considered (see II.E), we conjectured that the corresponding posterior distributions are not the same, and that we can obtain more information by considering outputs from the two previous posterior distributions.

This is confirmed by the outputs, as before the true parameter $\mathbf{p}^*$ is in the support of the a posteriori distribution. This technique allows us to gain information. This is an asset for real-world application.

VI.A.2. For a time of measurement 3600s with MC outputs

As we have seen in the previous subsubsection, considering two time gates provide more accurate approximation of the real parameter $\mathbf{p}^*$ by the use of the marginal distribution and when the outputs are exact $\mathbf{y}_{out} = \mathbf{M}(\mathbf{p}^*)$. In the real world application, we dispose of noisy outputs, $\mathbf{y}_{out} = \mathbf{M}(\mathbf{p}^*) + \varepsilon$, where ε is a noise coming from the system, the environment or the detector. In order to simulate real application, we will use the kinetic Monte-Carlo code 1 in the point model approximation. Then it will be interesting to compare the obtained mean and standard deviation, and the marginal distributions obtain with exact and MC measurements.

Thus, the outputs are

$$\mathbf{y}_{out} = \begin{pmatrix} \widehat{\mathbf{M}}_{MC,T_1} \\ \widehat{\mathbf{M}}_{MC,T_2} \end{pmatrix} = \begin{pmatrix} 0.14031 \\ 0.16059 \\ 0.20409 \\ 1.40461 \\ 3.39002 \\ 10.18181 \end{pmatrix} \tag{21}$$

Since the measurements associated with the two time gates are not correlated, the covariance

matrix is

$$\begin{pmatrix} \widehat{\mathbf{Cov}}_{MC,T_1} & (0) \\ (0) & \widehat{\mathbf{Cov}}_{MC,T_2} \end{pmatrix} =$$

$$\begin{pmatrix} 1.95455 \times 10^{-8} & 2.51849 \times 10^{-8} & 3.76928 \times 10^{-8} & & & \\ 2.51849 \times 10^{-8} & 3.80876 \times 10^{-8} & 6.795109 \times 10^{-8} & & (0) & \\ 3.76928 \times 10^{-8} & 6.795109 \times 10^{-8} & 1.41857 \times 10^{-7} & & & \\ & & & 1.96791 \times 10^{-6} & 7.52693 \times 10^{-6} & 3.04969 \times 10^{-5} \\ & (0) & & 7.52693 \times 10^{-6} & 3.43980 \times 10^{-5} & 1.57364 \times 10^{-4} \\ & & & 3.049685 \times 10^{-5} & 1.57364 \times 10^{-4} & 7.91919 \times 10^{-4} \end{pmatrix} \tag{22}$$

We have obtained the following mean and standard deviation for the MCMC sampling and MC point model measurements of duration 3600s:

$$\mathbb{E}[k_{eff}|\mathbf{y}_{out}] = 0.48829 \qquad \sqrt{\mathbb{E}[(k_{eff} - \mathbb{E}[k_{eff}|\mathbf{y}_{out}])^2|\mathbf{y}_{out}]} = 0.81588 \times 10^{-1} \tag{23}$$

$$\mathbb{E}[S|\mathbf{y}_{out}] = 74.173\ ms^{-1} \qquad \sqrt{\mathbb{E}[(S - \mathbb{E}[S|\mathbf{y}_{out}])^2|\mathbf{y}_{out}]} = 30.771\ ms^{-1} \tag{24}$$

$$\mathbb{E}[\varepsilon_C|\mathbf{y}_{out}] = 0.27443 \times 10^{-2} \qquad \sqrt{\mathbb{E}[(\varepsilon_C - \mathbb{E}[\varepsilon_C|\mathbf{y}_{out}])^2|\mathbf{y}_{out}]} = 0.10050 \times 10^{-2} \tag{25}$$

We compute the absolute error of the mean and standard deviation obtained with MCMC sampling with exact or MC outputs $\mathbf{y}_{out}$. The results are in the first columns of table III and IV providing a comparison of the different methods.

When it comes to evaluate the absolute error of the mean and standard deviation of $\mathbf{p}|\mathbf{y}_{out}$, we can claim these results are satisfying. So, with $\mathbf{y}_{obs,MC}$ and two time gates, we might estimate correctly the real parameters $\mathbf{p}^*$. It means that this method could be used in the experiments. The MC simulations are in the point model approximation. We could have used the Monte Carlo N-Particle Transport Code (MCNP) in order to have simulation that are closer to the real experiments. Using real data would be decisive.

In the figures 9 and 10, we showed the sampled marginal a posteriori distributions for T_1, T_2 and (T_1, T_2). As with exact and MC outputs, we observe that the maximum a posteriori is close to the real parameter $\mathbf{p}^*$ (represented by a large cross). So the MCMC method is efficient.

As for exact outputs, we observe that the estimation of $\mathbf{p}^*$ is better for T_1 than for T_2; and also that the estimation for (T_1, T_2) provide the best results. So the method is still interesting for real applications.

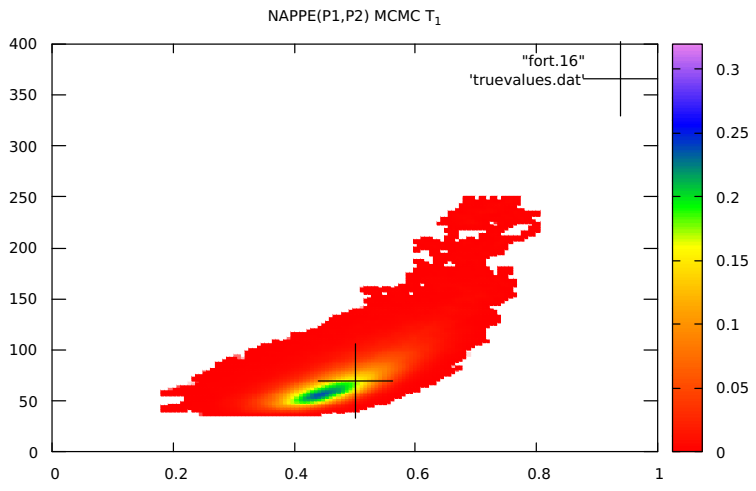

(a) $T_1 = \frac{1}{\alpha}$

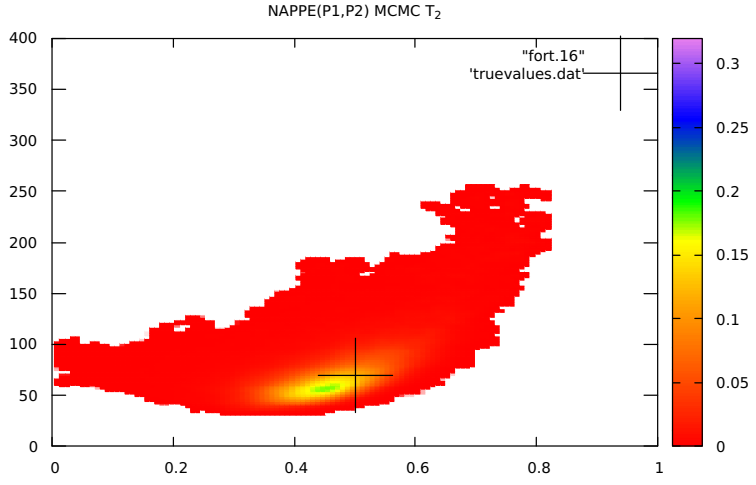

(b) $T_2 = \frac{10}{\alpha}$

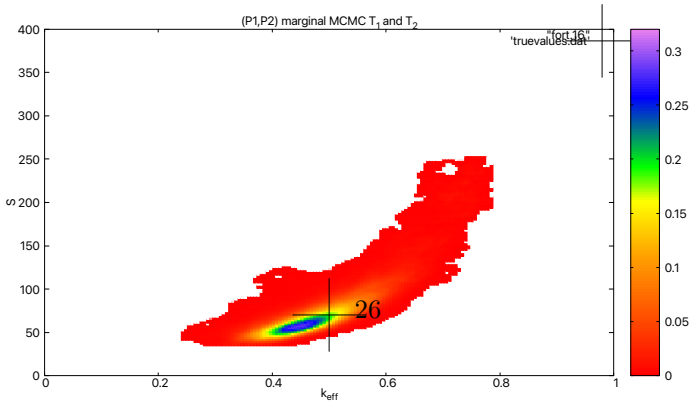

(c) (T_1, T_2)

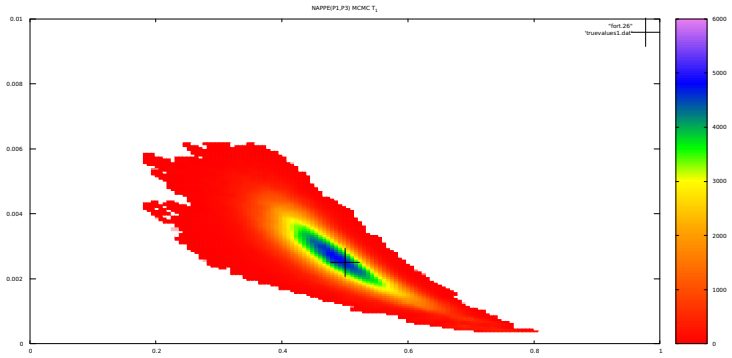

(a) $T_1 = \frac{1}{\alpha}$

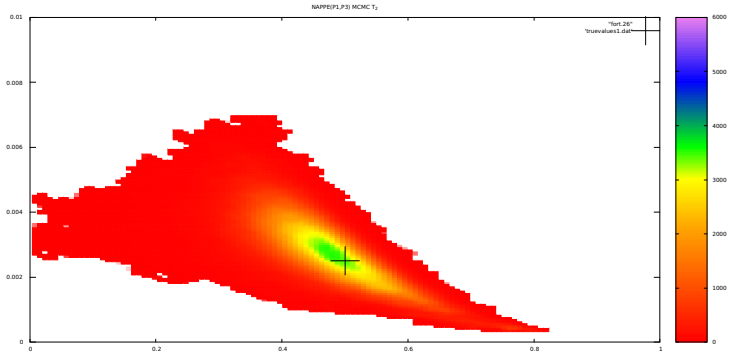

(b) $T_2 = \frac{10}{\alpha}$

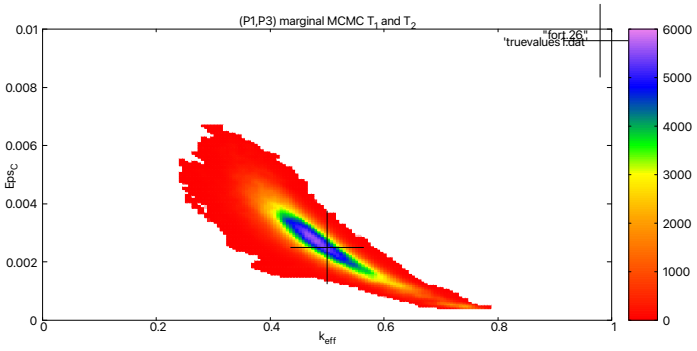

(c) (T_1, T_2)

Fig. 10. Marginal distribution of k_{eff} and ε_C for T_1, T_2 and (T_1, T_2) with MCMC sampling and MC outputs of 3600s

Now, we proved that the method is efficient with MC simulation during 3600s, we ask ourselves what method could be better in order to estimate $\mathbf{p}^*$ in the experiments. To do so, we compare the method using measurements during 7200s using T_1 and during 3600s using (T_1, T_2).

VI.A.3. For a time of measurement 7200s with exact outputs

In order to highlight the efficiency of the method using the time gate $T << \frac{1}{\alpha}$ for 7200s, we will compare the a posteriori distributions of using exact and MC outputs for a time of measurements 7200s.

The outputs are

$$\mathbf{y}_{out} = \mathbf{M}(\mathbf{p}^*, T_1) = \begin{pmatrix} 0.14043 \\ 0.16058 \\ 0.20382 \end{pmatrix} \tag{26}$$

Since the measurements associated with the two time gates are not correlated, the covariance matrix is

$$\mathbf{Cov}(\mathbf{p}^*, T_1) = \begin{pmatrix} 0.97816 \times 10^{-8} & 0.12588 \times 10^{-7} & 0.18819 \times 10^{-7} \\ 0.18819 \times 10^{-7} & 0.33904 \times 10^{-7} & 0.70761 \times 10^{-7} \\ 0.97816 \times 10^{-8} & 0.12588 \times 10^{-7} & 0.18819 \times 10^{-7} \end{pmatrix} \tag{27}$$

We have obtained the following mean and standard deviation for the MCMC sampling and exact measurements of duration 7200s:

$$\mathbb{E}[k_{eff}|\mathbf{y}_{out}] = 0.49004 \qquad \sqrt{\mathbb{E}[(k_{eff} - \mathbb{E}[k_{eff}|\mathbf{y}_{out}])^2|\mathbf{y}_{out}]} = 0.76988 \times 10^{-1} \tag{28}$$

$$\mathbb{E}[S|\mathbf{y}_{out}] = 73.265\ ms^{-1} \qquad \sqrt{\mathbb{E}[(S - \mathbb{E}[S|\mathbf{y}_{out}])^2|\mathbf{y}_{out}]} = 28.039\ ms^{-1} \tag{29}$$

$$\mathbb{E}[\varepsilon_C|\mathbf{y}_{out}] = 0.27313 \times 10^2 \qquad \sqrt{\mathbb{E}[(\varepsilon_C - \mathbb{E}[\varepsilon_C|\mathbf{y}_{out}])^2|\mathbf{y}_{out}]} = 0.96707 \times 10^{-3} \tag{30}$$

We can compute the absolute error of the mean and standard deviation obtained with MCMC sampling with exact outputs $\mathbf{y}_{out}$ for a duration of measurements of 3600s and 7200s. The results are in the second columns of table III and IV providing a comparison of the different methods.

Then we can evaluate the absolute error of the mean and standard deviation of $\mathbf{p}|\mathbf{y}_{out}$, we claim these results are satisfying. So, as expected, the estimation of $\mathbf{p}|\mathbf{y}_{out}$ with 7200s and T_1 is closer to $\mathbf{p}^*$ than with 3600s and (T_1, T_2), which make sense. We also notice that with

7200s and T_1 the standards deviation are larger than with 3600s and (T_1, T_2). Consequently, there is a compromise between having $\mathbb{E}[\mathbf{p}|\mathbf{y}_{out}]_{exact}$ close to $\mathbf{p}^*$ and having a small standard deviation $\sqrt{\mathbb{E}[(\mathbf{p} - \mathbb{E}[\mathbf{p}|\mathbf{y}_{out}])^2|\mathbf{y}_{out}]}_{exact}$. In the experiments, we want to have the smallest time of measurements that estimates $\mathbf{p}^*$ the best way which means $\mathbb{E}[\mathbf{p}|\mathbf{y}_{out}]_{exact}$ is the closest to $\mathbf{p}^*$ and having the smallest standard deviation $\sqrt{\mathbb{E}[(\mathbf{p} - \mathbb{E}[\mathbf{p}|\mathbf{y}_{out}])^2|\mathbf{y}_{out}]}_{exact}$.

Moreover, we can notice that the method with 7200s and (T_1, T_2) provide $\mathbb{E}[\mathbf{p}|\mathbf{y}_{out}]_{exact}$ in the same order of magnitude with T_1, and $\sqrt{\mathbb{E}[(\mathbf{p} - \mathbb{E}[\mathbf{p}|\mathbf{y}_{out}])^2|\mathbf{y}_{out}]}_{exact}$ is smaller with (T_1, T_2) (see equations 30 and 3.120-3.123 in [9]).

In the figures 11 and 12, we showed the sampled marginal a posteriori distributions for T_1, T_2 and (T_1, T_2). As with exact and MC outputs, we observe that the maximum a posteriori is close to the real parameter $\mathbf{p}^*$ (represented by a large cross). So the MCMC method is efficient.

As for exact outputs of duration 3600s, we observe that the estimation of $\mathbf{p}^*$ is better for T_1 than for T_2; and also that the estimation for (T_1, T_2) provide the best results. This means the method is still interesting for real applications.

VI.A.4. For a time of measurement 7200s and MC outputs

As suggested by the previous subsubsection, we want to know whether it is worth to wait 7200s and use one time gate $T_{1,7200s}$ or wait 3600s and use two time gates $(T_{1,3600s}, T_{2,3600s})$.

So we computed the simple moments and the associated covariance matrix for a time of measurements of 7200s.

For $T_1 << \frac{1}{\alpha}$, we obtained the following outputs

$$\mathbf{y}_{out} = \widehat{\mathbf{M}}_{MC,T_1} = \begin{pmatrix} 0.14024 \\ 0.16035 \\ 0.20355 \end{pmatrix} \tag{31}$$

We obtained the following covariance matrix

$$\widehat{\mathbf{Cov}}_{MC,T_1} = \begin{pmatrix} 9.75801 \times 10^{-9} & 1.25583 \times 10^{-8} & 0.87755 \times 10^{-8} \\ 1.25583 \times 10^{-8} & 1.89719 \times 10^{-8} & 3.38247 \times 10^{-8} \\ 0.87755 \times 10^{-8} & 3.38247 \times 10^{-8} & 7.05523 \times 10^{-8} \end{pmatrix} \tag{32}$$

We have obtained the following mean and standard deviation for the MCMC sampling and

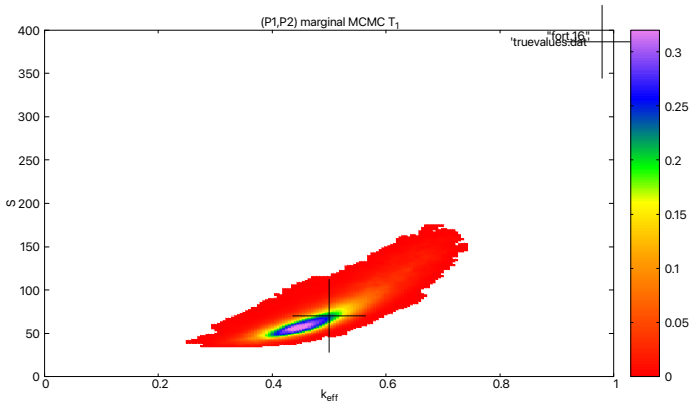

(a) $T_1 = \frac{1}{\alpha}$

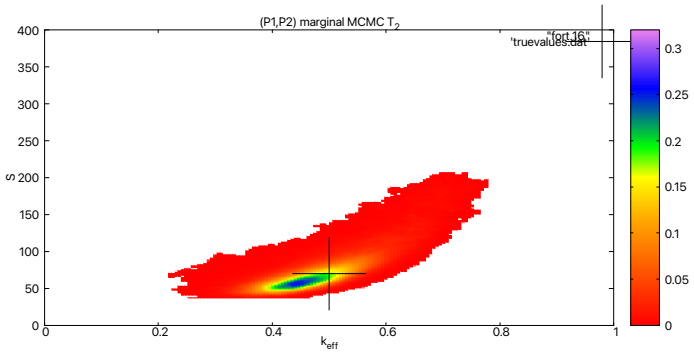

(b) $T_2 = \frac{10}{\alpha}$

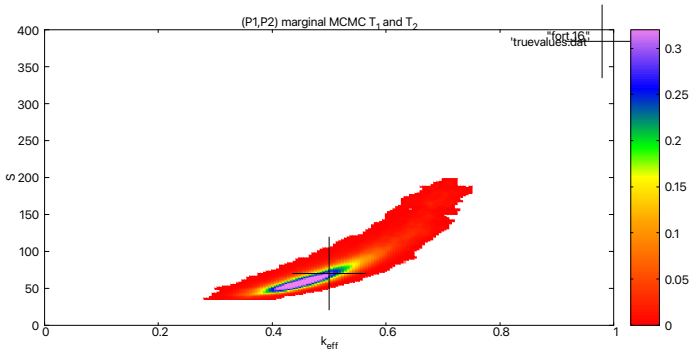

(c) (T_1, T_2)

Fig. 11. Marginal distribution of k_{eff} and S for T_1, T_2 and (T_1, T_2) with MCMC sampling and exact outputs of 7200s

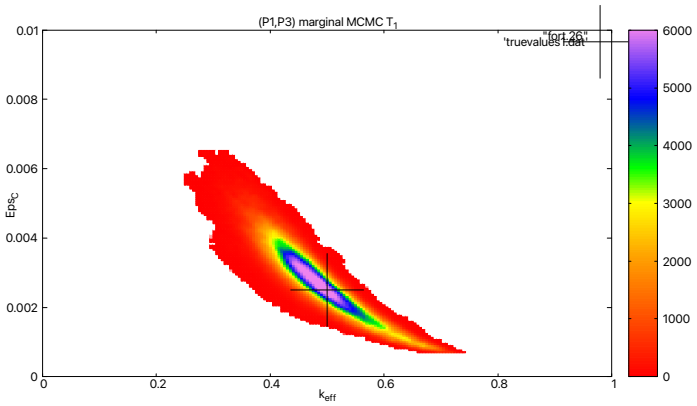

(a) $T_1 = \frac{1}{\alpha}$

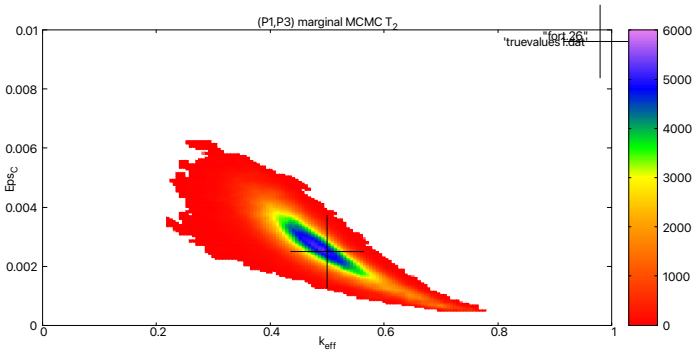

(b) $T_2 = \frac{10}{\alpha}$

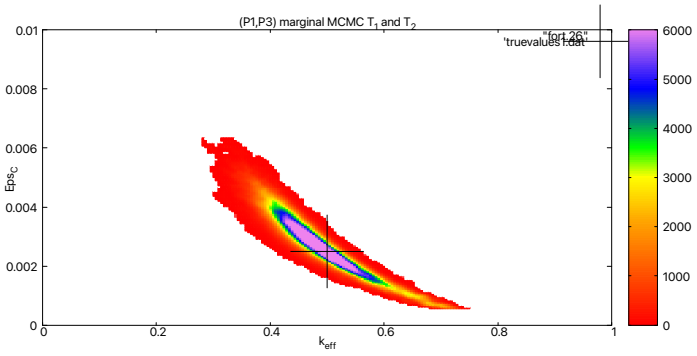

(c) (T_1, T_2)

Fig. 12. Marginal distribution of k_{eff} and ε_C for T_1, T_2 and (T_1, T_2) with MCMC sampling and exact outputs of 7200s

MC point model measurements of duration 7200s:

$$\mathbb{E}[k_{eff}|\mathbf{y}_{out}] = 0.48260 \qquad \sqrt{\mathbb{E}[(k_{eff} - \mathbb{E}[k_{eff}|\mathbf{y}_{out}])^2|\mathbf{y}_{out}]} = 0.72519 \times 10^{-1} \tag{33}$$

$$\mathbb{E}[S|\mathbf{y}_{out}] = 70.455\ ms^{-1} \qquad \sqrt{\mathbb{E}[(S - \mathbb{E}[S|\mathbf{y}_{out}])^2|\mathbf{y}_{out}]} = 23,407\ ms^{-1} \tag{34}$$

$$\mathbb{E}[\varepsilon_C|\mathbf{y}_{out}] = 0.28212 \times 10^{-2} \qquad \sqrt{\mathbb{E}[(\varepsilon_C - \mathbb{E}[\varepsilon_C|\mathbf{y}_{out}])^2|\mathbf{y}_{out}]} = 0.96013 \times 10^{-3} \tag{35}$$

We can compute the absolute error of the mean and standard deviation obtained with MCMC sampling with exact or MC outputs $\mathbf{y}_{out}$. The results are in the third columns of table III and IV providing a comparison of the different methods.

The absolute error of the mean and standard deviation of $\mathbf{p}|\mathbf{y}_{out}$ are really satisfying. The order of magnitude are interesting for the applications. A deeper analysis will be performed in the discussion.

When the time of measurements is greater, the simple moments $\mathbf{y}_{out}$ are better valued. We look at the marginal distributions for further analysis.

In the figures 13 and 14, we represent the a posteriori distributions. As with exact and MC outputs, we observe that the maximum a posteriori is close to the real parameter $\mathbf{p}^*$ (represented by a large cross).

As for exact outputs, we observe that the estimation of $\mathbf{p}^*$ is better for T_1 than for T_2; and also that the estimation for (T_1, T_2) provide the best results. In this context, the method is still interesting for real measurements.

The objective of these computations was to compare the estimation of $\mathbf{p}^*$ with MC simulations of duration 3600s and two times gates $(T_{1,3600s}, T_{2,3600s})$ and with MC simulations of duration 7200s and one time gate $T_{1,7200s}$. This will be discussed in the next section.

VII. DISCUSSION

VII.A. Use of the MCMC sampling with exact and MC measurements during 3600s

As we have seen in the parts VI.A.1 and VI.A.2, the estimation of $\mathbf{p}|\mathbf{y}_{out}$ is satisfying : $\mathbb{E}[\mathbf{p}|\mathbf{y}_{out}]_{exact}$ is close to $\mathbf{p}^*$ and $\sqrt{\mathbb{E}[(\mathbf{p} - \mathbb{E}[\mathbf{p}|\mathbf{y}_{out}])^2|\mathbf{y}_{out}]}_{exact}$ is small enough. We recall the absolute errors on the mean and the standard deviation are in the first columns of tables III and IV.

On the a posteriori distribution, we can see that $\mathbf{p}^*$ is close to the Maximum A Posteriori (MAP) of the two marginal distributions. This is satisfying, if there is a better approximation we need to specify in which meaning.

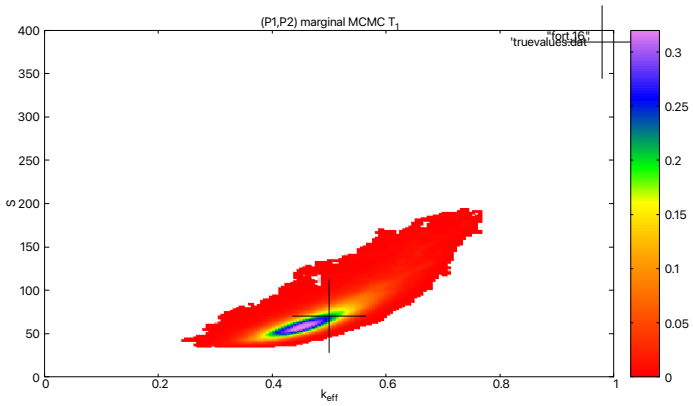

(a) $T_1 = \frac{1}{\alpha}$

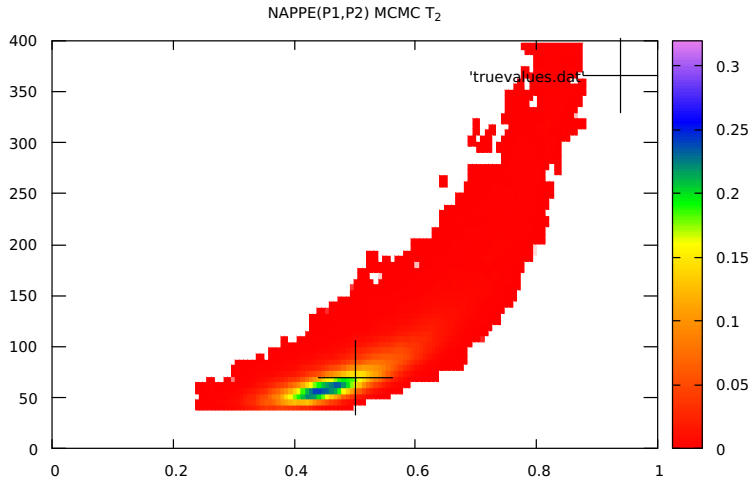

(b) $T_2 = \frac{10}{\alpha}$

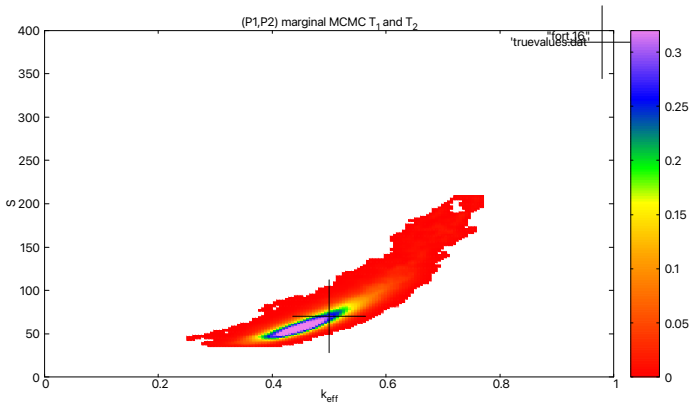

(c) (T_1, T_2)

Fig. 13. Marginal distribution of k_{eff} and S for T_1, T_2 and (T_1, T_2) with MCMC sampling and MC outputs of 7200s

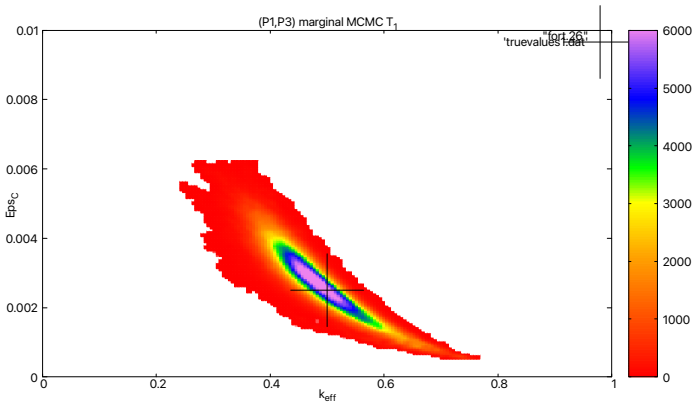

(a) $T_1 = \frac{1}{\alpha}$

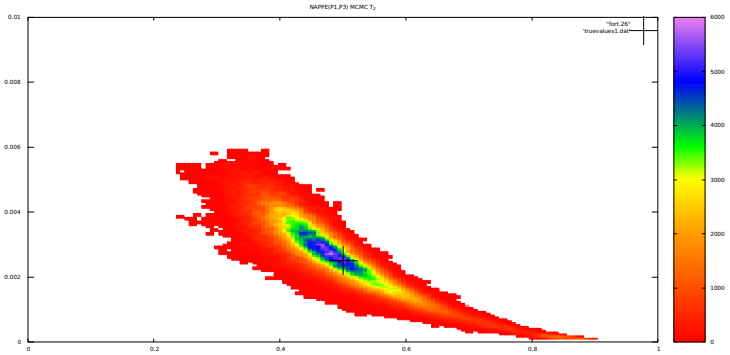

(b) $T_2 = \frac{10}{\alpha}$

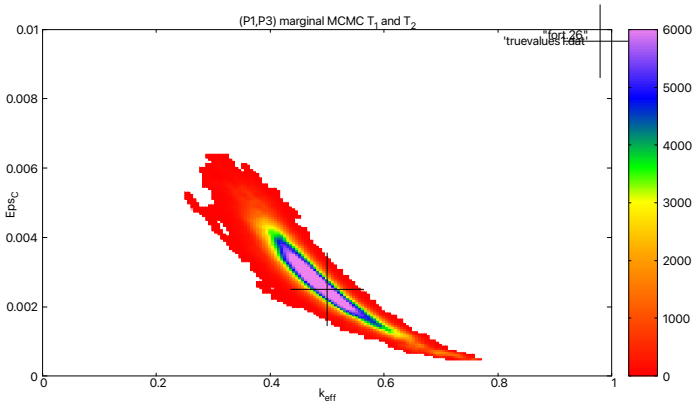

(c) (T_1, T_2)

Fig. 14. Marginal distribution of k_{eff} and ε_C for T_1, T_2 and (T_1, T_2) with MCMC sampling and MC outputs of 7200s

By looking at the marginal distribution with $T_1 = \frac{1}{\alpha}$, $T_2 = \frac{10}{\alpha}$ and (T_1, T_2) we observe that the MAP is better approximated with T_1 than with T_2. We need to clarify if is better to wait 7200s and only use T_1 or wait 3600s and use (T_1, T_2).

To do so, we have to compare at first the results with exact outputs. This will provide an absolute reference for comparison.

VII.B. Use of the MCMC sampling with exact measurements during 3600s with (T_1, T_2) and 7200s with T_1

As suggested by the previous subsection, we want to compare the a posteriori distributions with exact outputs for 3600s with (T_1, T_2) and 7200s with T_1. So we take into account, the results of the part VI.A.3. We recall the absolute errors on the mean and the standard deviation are in the second columns of tables III and IV. With 7200s with T_1, the mean is closer to $\mathbf{p}^*$ than with 3600s with (T_1, T_2). The standard deviation is also larger.

VII.C. Use of the MCMC sampling with exact and MC measurements during 7200s

Now, we compare the results with exact and MC outputs for a time gate T_1 and a time of measurements of 7200s. We recall the absolute errors on the mean and the standard deviation are in the third columns of tables III and IV.

The results of VI.A.4 suggest that the estimation of the mean and the standard deviation are satisfying. The absolute error on the means are of the same order of magnitude as for the comparison of the a posteriori distribution with exact and MC outputs for 3600s and two time gates. But, the absolute error on the standard deviation is more satisfying than in the case for 3600s and two time gates.

The a posteriori distribution also suggests a good approximation of $\mathbf{p}^*$ with a clear peak.

These results of this subsection and the previous one enable us to draw a qualitative and quantitative comparison of the method with 3600s and (T_1, T_2) and 7200s and $T1$: in this case, if we want to be precise we will wait 7200s and use one time gate $T << \frac{1}{\alpha}$.

When lacking of time, the method with 3600s of measurements and two time gates is still satisfying.

Observations method / Absolute error on $\mathbb{E}[\mathbf{p}\|\mathbf{y}_{out}]$	Exact vs MC 3600s (T_1, T_2)	Exact 3600s (T_1, T_2) vs Exact 7200s T_1	Exact vs MC 7200s T_1
k_{eff}	$8,0300 \times 10^{-3}$	$1,4290 \times 10^{-2}$	$7,4400 \times 10^{-3}$
S	$4,7320\ ms^{-1}$	$2,5030\ ms^{-1}$	$2,8100\ ms^{-1}$
ε_C	$8,9500 \times 10^{-5}$	$1,0780 \times 10^{-4}$	$8,9900 \times 10^{-5}$

TABLE III
Absolute error on the mean $\mathbb{E}[\mathbf{p}|\mathbf{y}_{out}]$ by considering the method Exact vs MC 3600s (T_1, T_2), then Exact 3600s (T_1, T_2) vs Exact 7200s T_1, and finally Exact vs MC 7200s T_1

Observations method / Absolute error on $\sqrt{\mathbb{E}[(\mathbf{p} - \mathbb{E}[\mathbf{p}\|\mathbf{y}_{out}])^2\|\mathbf{y}_{out}]}$	Exact vs MC 3600s (T_1, T_2)	Exact 3600s (T_1, T_2) vs Exact 7200s T_1	Exact vs MC 7200s T_1
k_{eff}	$1,1836 \times 10^{-2}$	$7,7400 \times 10^{-4}$	$4,4690 \times 10^{-3}$
S	$10.115\ ms^{-1}$	$4,1620\ ms^{-1}$	$4,6320\ ms^{-1}$
ε_C	$7,9120 \times 10^{-5}$	$3,3300 \times 10^{-6}$	$6,9400 \times 10^{-6}$

TABLE IV
Absolute error on the standard deviation $\sqrt{\mathbb{E}[(\mathbf{p} - \mathbb{E}[\mathbf{p}|\mathbf{y}_{out}])^2|\mathbf{y}_{out}]}$ by considering the method Exact vs MC 3600s (T_1, T_2), then Exact 3600s (T_1, T_2) vs Exact 7200s T_1, and finally Exact vs MC 7200s T_1

VII.D. Use of the MCMC sampling with MC measurements during 3600s with (T_1, T_2) and 7200s with T_1

Finally, we can draw a clear comparison with the MCMC method with MC measurements during 3600s with (T_1, T_2) and 7200s with T_1.

First, for 7200s with T_1 with exact outputs we observed by VII.B that $\mathbb{E}[\mathbf{p}|\mathbf{y}_{out}]_{exact}$ estimate well $\mathbf{p}^*$ and $\sqrt{\mathbb{E}[(\mathbf{p} - \mathbb{E}[\mathbf{p}|\mathbf{y}_{out}])^2|\mathbf{y}_{out}]}_{exact}$ is large. On the other hand, for 3600s with (T_1, T_2) with exact output we observe that the estimation $\mathbb{E}[\mathbf{p}|\mathbf{y}_{out}]_{exact}$ is less satisfying than with the previous method but $\sqrt{\mathbb{E}[(\mathbf{p} - \mathbb{E}[\mathbf{p}|\mathbf{y}_{out}])^2|\mathbf{y}_{out}]}_{exact}$ is smaller.

We recall the order magnitude of the absolute errors for the mean, in the table III, and the standard deviation, in the table IV.

Firstly, we know that the estimation of the mean $\mathbb{E}[\mathbf{p}|\mathbf{y}_{out}]$ is better with T_1 and 7200s of measurements than with (T_1, T_2) and 3600s of measurements. The standard deviation $\sqrt{\mathbb{E}[(\mathbf{p} - \mathbb{E}[\mathbf{p}|\mathbf{y}_{out}])^2|\mathbf{y}_{out}]}$ is also larger when we use T_1 and 7200s of measurements. On the second table, we see that the absolute error between the standard deviation of the a posteriori distribution are small, these are smaller than the error between the results of the exact outputs or MC outputs for 3600s and (T_1, T_2), the same goes for 7200s and T_1, what is satisfying.

Secondly, we obtain the same orders of magnitude for the mean $\mathbb{E}[\mathbf{p}|\mathbf{y}_{out}]$ with exact and

MC outputs for 3600s and (T_1, T_2) or with exact and MC outputs for 7200s and T_1. This recalls us the efficiency of the MCMC method with MC measurements. However, since the exact method for 7200s measurements and T_1 is close to $\mathbf{p}^*$ it will be more interesting to use this last method, when there is no time constraint for the measurements. Thirdly, we know that the standard deviation $\sqrt{\mathbb{E}[(\mathbf{p} - \mathbb{E}[\mathbf{p}|\mathbf{y}_{out}])^2|\mathbf{y}_{out}]}$ is greater for exact outputs of duration 7200s with T_1. On the table, we see that the absolute error on the standard deviation of the a posteriori distribution is one order of magnitude smaller in the case with 7200s and T_1 than in the case with 3600s and (T_1, T_2). When we sum the absolute error of the standard deviation on the comparison with exact outputs for 3600s with (T_1, T_2) and for 7200s with T_1 and the standard deviation with exact and MC outputs for 7200s with T_1, the results is still more satisfying than with exact and MC outputs for 3600s and (T_1, T_2). To sum up this paragraph, we can say that the absolute error on the standard deviation of the a posteriori distribution is satisfying but perfectible.

To sum up, we have two arguments in favour of the use of the method with MC measurements and 7200s with T_1 and one in favour of the use of the method with 3600s and (T_1, T_2). An optimized method would have a smaller standard deviation with exact output with T_1 and a large time of measurements, but we already have a really satisfying estimation of $\mathbb{E}[\mathbf{p}|\mathbf{y}_{out}]$ and the absolute error on the standard deviation $\sqrt{\mathbb{E}[(\mathbf{p} - \mathbb{E}[\mathbf{p}|\mathbf{y}_{out}])^2|\mathbf{y}_{out}]}$ is also really satisfying.

In the figures 15, we observe that the peak of the marginal distribution of k_{eff} and S is more pronounced for a time of measurement of 7200s and $\mathbf{p}^*$ is more probable than when we consider a time of measurement of 3600s and (T_1, T_2). In the figures 16, by considering the marginal distribution of k_{eff} and ε_C the previous statement is more accurate.

To conclude this comparison, we recommend to use the largest time of measurements and use T_1 when there is no time limit. Nonetheless, when there is only one hour to do the measurements, we recommend to use the method with two time gates (T_1, T_2).

VII.E. About an optimized method

We ask ourselves when it is possible to have an optimized estimation of $\mathbf{p}^*$ with the mean $\mathbb{E}[\mathbf{p}|\mathbf{y}_{out}]$ and the standard deviation $\sqrt{\mathbb{E}[(\mathbf{p} - \mathbb{E}[\mathbf{p}|\mathbf{y}_{out}])^2|\mathbf{y}_{out}]}$. We already have a method with a really good estimation of the mean. Getting a smaller standard deviation might be an improvement.

Numerically, we observed that the convergence of $\widehat{\mathbf{M}}$ to $\mathbf{M}(\mathbf{p}^*)$ is achieved for 3600s and 7200s of measurements. So for a fixed time gate T, there is no difference of considering $\widehat{\mathbf{M}}$ with 3600s and 7200s. The covariance matrix of the measurements being different, and so the corresponding a posteriori distribution is not the same $\mathbb{P}(\mathbf{p}|\widehat{\mathbf{M}})$. Knowing this fact, it would be interesting to optimize $\mathbb{P}(\mathbf{p}|\widehat{\mathbf{M}})$ by the use of the covariance matrix of the measurements in order to obtain an

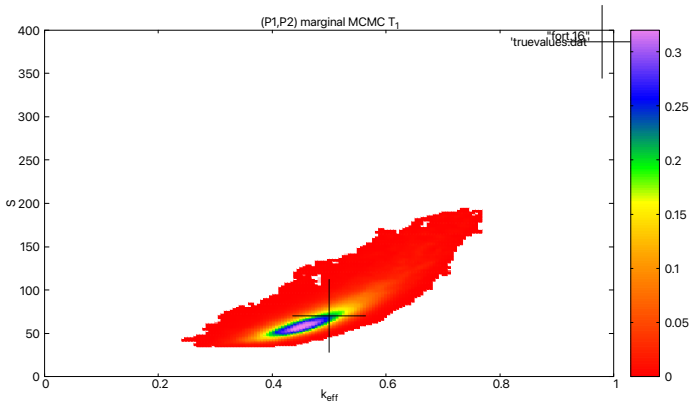

(a) $T_1 = \frac{1}{\alpha}$ with a time of measurements of 7200s

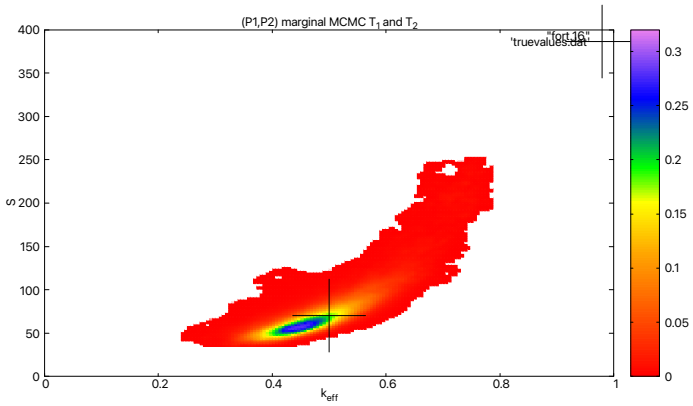

(b) (T_1, T_2) with a time of measurements of 3600s

Fig. 15. Marginal distribution of k_{eff} and S for T_1 with a time of measurements of 7200s and (T_1, T_2) with a time of measurements of 3600s with MCMC sampling

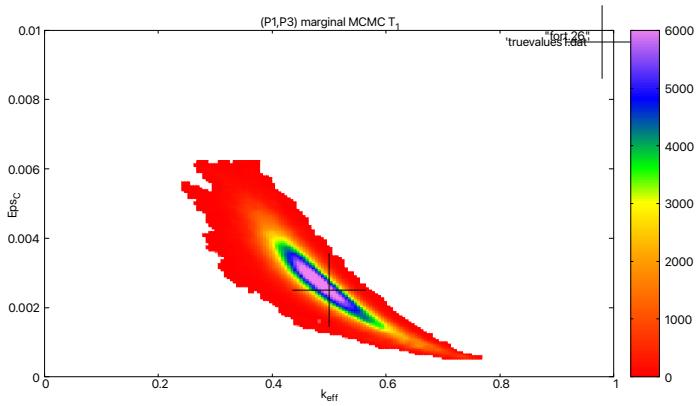

(a) $T_1 = \frac{1}{\alpha}$ with a time of measurements of 7200s

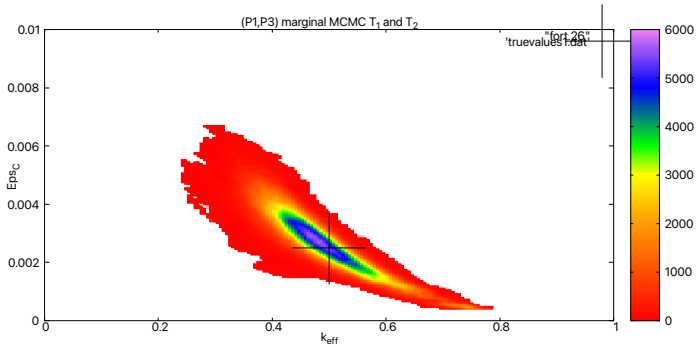

(b) (T_1, T_2) with a time of measurements of 3600s

Fig. 16. Marginal distribution of k_{eff} and ε_C for T_1, with a time of measurements of 7200s and (T_1, T_2) with a time of measurements of 3600s with MCMC sampling

accurate mean with a smaller standard deviation.

VIII. CONCLUSION

In this study, we settled the forward problem of the neutron counting distribution in the point model approximation. We explained what the outputs $\mathbf{y}_{out}$ are and how the measurements are made. We did some estimations of the measurements $\widehat{\mathbf{M}}$ using a kinetic Monte-Carlo code. Then, we defined the Bayesian inverse problem of getting the a posteriori distribution of $\mathbf{p}$, the parameters of the neutronic system, knowing the outputs: $\mathbb{P}(\mathbf{p}|\mathbf{y}_{out})$. In order to sample this non-trivial distribution, we introduced the Markov Chain Monte Carlo with Covariance Matrix Adaptation (MCMC with CMA) algorithm. We presented a set of test-cases in order to show how this a posteriori distribution is degenerate which justify the use of the MCMC sampled with CMA. The algorithm works in around 10min, which is interesting for real-time use. In order to get a better sampling of the distribution of interest, we introduced a new method using two time gates (T_1, T_2) rather than just a simple time gates T_1 or T_2. The use of two time gates provide a better sampling of the a posteriori distribution of the parameters knowing the outputs. Moreover, we analysed the impact on the sampling of the use of exact or Monte-Carlo outputs with a time of measurements of 3600s and 7200s. Thus, we compared the use of (T_1, T_2) with 3600s of measurements and T_1 with 7200s of measurements. We obtained a better approximation of the mean $\mathbb{E}[\mathbf{p}|\mathbf{y}_{out}]$ and the standard deviation $\sqrt{\mathbb{E}[(\mathbf{p} - \mathbb{E}[\mathbf{p}|\mathbf{y}_{out}])^2|\mathbf{y}_{out}]}$ for the second option. The peak of the a posteriori distribution are more pronounced with 7200s and T_1 than with 3600s and (T_1, T_2). The peak is also closer to the real parameter we want to estimate. In that case, it is more interesting to use T_1 and wait 7200s for a better study of the a posteriori distribution of the parameters of the system knowing the measurements.

There is still room for improvement regarding the sampling: the best MCMC method would provide the closest mean to $\mathbf{p}^*$ and the smallest standard deviation. To do so, we can do optimization on $\mathbb{P}(\mathbf{p}|\widehat{\mathbf{M}})$ in order to get the result. More precisely, we can compute the eigenvalues of the covariance matrix of the measurements and use it. Moreover, four parameters probability density function of Maximum A Posteriori estimates are provided in the technical report [4]. Using two time gates can give four parameters, which could be a good comparison with Lawrence Livermore National Laboratory's report. In real experiments, time gate width dependency is more complex and dead-time effects occurs [12]. For short time gates, as used in the article, dead-time effects are really difficult to take into account, so the method presented should be reconsidered.

REFERENCES

[1] R. Dierckx and W. Hage, "Neutron Signal Multiplet Analysis for the Mass Determination of Spontaneous Fission Isotopes," *Nuclear Science and Engineering*, **85**, *4*, 325 (1983)URL https://doi.org/10.13182/NSE83-3.

[2] D. Cifarelli and W. Hage, "Models for a three-parameter analysis of neutron signal correlation measurements for fissile material assay," *Nuclear Instruments and Methods in Physics Research Section A: Accelerators, Spectrometers, Detectors and Associated Equipment*, **251**, *3*, 550 (1986)URL https://doi.org/10.1016/0168-9002(86)90651-0.

[3] T. Sullivan, *Introduction to Uncertainty Quantification*, Springer International Publishing (2015)URL https://doi.org/10.1007/978-3-319-23395-6.

[4] S. Walston, J. Candy, D. Chambers, H. Chandrasekaran, and N. Snyderman, "Real-Time Characterization of Special Nuclear Materials," **LLNL-TR-676944** (2015)URL https://www.osti.gov/biblio/1234623.

[5] P. Humbert, "Simulation and Analysis of List Mode Measurements on SILENE Reactor," *Journal of Computational and Theoretical Transport*, **47**, *4-6*, 350 (2018)URL https://doi.org/10.1080/23324309.2018.1477802.

[6] R. P. Feynman, F. de Hoffmann, and R. Serber, "Statistical fluctuations in the water boiler and the dispersion of neutrons emitted per fission," *Los Alamos National Laboratory*, **LA-101**, 22 (1944)URL http://lib-www.lanl.gov/cgi-bin/getfile?00349748.pdf.

[7] J. E. M. Saxby, A. K. Prinja, and M. D. Eaton, "Energy Dependent Transport Model of the Neutron Number Probability Distribution in a Subcritical Multiplying Assembly," *Nuclear Science and Engineering*, **189**, *1*, 1 (2018)URL https://doi.org/10.1080/00295639.2017.1367569.

[8] G. I. Bell and S. Glasstone, *Nuclear Reactor Theory*, Van Nostrand Reinhold Company (1970)URL https://www.osti.gov/biblio/4074688.

[9] C. Houpert, "Inverse problem for stochastic neutronics," Phd thesis, École polytechnique, IP Paris (2022)URL http://www.theses.fr/2022IPPAX124/document.

[10] I. Pazsit and L. Pal, *Neutron Fluctuations: A Treatise on the Physics of Branching Processes*, Elsevier Ltd (2008).

[11] S. L. N. Tsoulfanidis, *Measurements & Detection of radiation 4^{th} edition*, CRC Press (2015)URL https://doi.org/10.1201/b18203.

[12] Y. N. Erez Gilad and C. Dubi, "Dead time corrections on the Feynman-Y curve using the backward extrapolation method," *Journal of Nuclear Science and Technology*, **55**, *2*, 229 (2018)URL https://www.tandfonline.com/doi/epdf/10.1080/00223131.2017.1394231?needAccess=true.

[13] A. F. Voter, *Introduction to the Kinetic Monte Carlo Method*, Springer Netherlands, Dordrec (2007)URL https://helper.ipam.ucla.edu/publications/matut/matut_5898_preprint.pdf.

[14] A. Tarantola, *Inverse Problem Theory and Methods for Model Parameter Estimation*, SIAM (2005)URL https://www.geologie.ens.fr/~jolivet/Research_files/Tarantola.pdf.

[15] C. Andrieu and J. Thoms, "A tutorial on adaptive MCMC," *Stat Comput*, **18**, 343–373 (2008)URL https://people.eecs.berkeley.edu/~jordan/sail/readings/andrieu-thoms.pdf.

[16] H. Haario, E. Saksman, and J. Tamminen, "An Adaptive Metropolis algorithm," *Bernoulli*, **7**, *2*, 223 (2001)URL https://projecteuclid.org/journals/bernoulli/volume-7/issue-2/An-adaptive-Metropolis-algorithm/bj/1080222083.full.

[17] C. Mueller, "Exploring the common concepts of adaptive MCMC and Covariance Matrix Adaptation schemes," A. Auger, J. L. Shapiro, L. D. Whitley, and C. Witt (Editors), *Theory of Evolutionary Algorithms, 05.09. - 10.09.2010*, vol. 10361 of *Dagstuhl Seminar Proceedings*, 1–10, Schloss Dagstuhl - Leibniz-Zentrum für Informatik, Germany (2010)URL https://drops.dagstuhl.de/storage/16dagstuhl-seminar-proceedings/dsp-vol10361/DagSemProc.10361.3/DagSemProc.10361.3.pdf.

[18] A. Gelman, G. Roberts, and W. R. Gilks, "Efficient Metropolis Jumping Rules," *Bayesian Statistics*, **5**, 599 (1996).

[19] J. Garnier, C. Houpert, and P. Humbert, "Inverse Problems for Stochastic Neutronics," *Eccomas Proceedia UNCECOMP*, 63–74 (2021)URL https://www.eccomasproceedia.org/conferences/thematic-conferences/uncecomp-2021/8022.

[20] J. Verbeke, "Neutron Multiplicity Counting: Credible Regions for Reconstruction Parameters," *Nuclear Science and Engineering*, **182**, *4*, 481 (2016)URL https://doi.org/10.13182/NSE15-35.